Host protection to intestinal worm infections: the importance of activated and armed innate effector cells at the host parasite interface.

Anupama Ariyaratne[1], Sang Yong Kim[2], Stephen M. J. Pollo[3], Mayara de Cassia Luzzi[1,4], Joel Bowron[1], Edina Szabo[1], James D. Wasmuth[3], Meera G. Nair[2], Constance A. M. Finney[1]

[1]Department of Biological Sciences, Faculty of Science, University of Calgary, Calgary, Alberta, Canada.

[2] School of Medicine, University of California Riverside, California, USA.

[3] Department of Ecosystems and Public Health, Faculty of Veterinary Medicine, University of Calgary, Alberta, Canada.

[4] Department of Veterinary Pathology, São Paulo State University - UNESP, Jaboticabal, SP, Brazil

Corresponding Author: Constance A. M. Finney, constance.finney@ucalgary.ca, Faculty of Science, Department of Biological Sciences, University of Calgary, 2500 University Drive N.W., Calgary, Alberta, Canada.

Keywords: parasitic worm infections, nematodes, granuloma, innate immunity, antibody responses

ABSTRACT

Intestinal roundworms cause chronic debilitating disease in animals, including humans. A lack of effective vaccines and the emergence of widespread drug resistance only increase the need to better understand parasite clearance mechanisms within the host. *Heligmosomoides polygyrus* larvae induce a strong intestinal granuloma response within their murine host, which has been associated with resistance. Immune cells, mostly alternatively activated macrophages and eosinophils, accumulate around the tissue encysted parasites to immobilize and damage/kill developing worms. In a one dose (bolus) experimental infection, infected C57Bl/6 mice are unable to clear parasites which results in chronic infection with high worm burdens. However, using a frequent dose trickle model of infection, we, like others, have found that C57Bl/6 mice can clear infection. We found that the clearance is associated with higher granuloma numbers, but no changes in systemic/intestinal Th2 responses. Within the granulomas, we found that myeloid cells had a different transcriptional profile in each of the infected groups, and that high IgG1, but not IgG2c, IgA or IgE, levels were observed around the larvae of only trickle-infected mice. Our results highlight the importance of the granuloma in the host's ability to clear *H. polygyrus* and emphasise the need to study this key tissue in more depth, rather than using correlates such as general intestinal or systemic responses.

AUTHOR'S SUMMARY

Despite decades of research on intestinal parasitic worms, we are still unable to clearly point to why so many people (approximately 1.8 billion) and most livestock/wild animals are infected with these parasites. We have made progress in understanding how the immune system responds to parasitic worms, and how these parasites manipulate our immune system. However, identifying effective clearance mechanisms is complex and context dependent. We have used a model of trickle infection (multiple low doses of parasites) to simulate how people/animals get infected in the real world. Using this model, we have identified the host/parasite interface (the granuloma) within the intestinal tissue to be key in determining the host's ability to clear worms. Specific gene expression signatures in granuloma immune cells and the presence/absence of antibodies within the granuloma are key factors associated with parasite clearance. Surprisingly, more common identifiers of parasitic worm infections (increased serum antibody levels and/or generalized immune markers) did not associate with protection. These novel findings contribute to a better understanding of the mechanisms underlying effective parasitic worm clearance.

INTRODUCTION

Gastrointestinal nematodes are parasites adept at causing chronic recurring infections. Hosts mount a strong immune response to these parasites, essential to control worm burden and host tissue damage. However, the efficacy of the response is dependent on genetics, infection dynamics and environment.

Heligmosomoides polygyrus is an enteric nematode parasite of mice [1],[2]. Ingested larvae encyst in the host intestinal wall and mature into adults that escape into the lumen. Adults remain in the intestinal lumen for the duration of infection. *H. polygyrus* tissue dwelling stages cause the release of alarmins from epithelial cells as they damage the intestinal wall [3]–[5]. Alarmin-activated innate lymphoid cells and Th2 polarized $CD4^+$ T cells produce Th2 cytokines [6]–[9] which promote innate immune cell influx to the intestine [2],[6],[10]. The accumulation of immune cells is referred to as a granuloma [7],[11],[12]. Increased granuloma size and number are associated with increased resistance to nematodes [13].

Within the granuloma, the host response focuses on damaging or killing the parasitic nematodes, as well as healing the damage caused by the growing worm (reviewed in [14]). Eliminating tissue stage parasites is thought to rely on antibody dependent cell mediated cytotoxicity (ADCC) by macrophages and eosinophils [7],[15],[16], the main cellular players within the granuloma. Antibodies are key to this process. Resistant

strains of mice have been shown to develop faster and more intense parasite specific antibody responses following *H. polygyrus* infections, as compared to susceptible strains, where isotypes IgG_1, IgA and IgE have been linked to worm clearance [2],[17],[18]. Passive transfer of serum, and specifically IgG_1, from infected mice results in decreased adult worm burden and fecundity [19]–[22]. *H. polygyrus* adult numbers are increased in infected mice lacking IgA [23]. IgG_1 and IgE have also been negatively correlated with worm survival across different strains of mice [24]–[26].

Alternatively activated macrophages (AAMs) isolated from *H. polygyrus*-induced granulomas have increased surface levels of FcγRs as well as complement receptor CD11b and surface binding of IgG_1 and IgG_3 [27]. However, the exact mechanisms responsible for parasite adherence and killing remain controversial. *In vitro* observations have yet to be validated *in vivo*. For example, the CD11b receptor on bone marrow derived macrophages can directly bind *H. polygyrus* larvae using complement 3 when cultured with immune serum. *In vitro*, after adhering to the larvae via the CD11b-C3 interaction [27], FcγR1 on macrophages can interact with parasite bound $IgG_{2a/c}$ (but not IgG_1) antibodies to immobilize the larvae [28]. However, this binding does not reduce the infectivity of larvae *in vivo* [27]. In contrast, mice vaccinated with *H. polygyrus* excretory/secretory products (HES) are protected from chronic infection as a result of the IgG_1 response [5]. IgG_1 antibodies are thought to bind and neutralize parasite excretory secretory products, that in unvaccinated mice are able to interfere with the

106 functions of protective innate immune cells [5]. However, passive transfer of purified
107 IgG_1 did not induce sterile immunity suggesting that other mechanisms are at play [5].
108 As well as being involved in parasite damage and death, AAMs and eosinophils are both
109 also involved in host tissue repair [14]. AAMs produce immunoregulatory and wound
110 healing molecules [29],[30] which promote extracellular matrix (ECM) deposition during
111 helminth infections [31]–[34]. *H. polygyrus* infections induce Ym1 and RELM-α secretion
112 from AAMs [2], both linked with the wound healing phenotype [35]. Eosinophils also
113 produce RELM-α [36], TGF- α, TGF-β and fibroblast growth factors [37]–[39]. In addition,
114 Arginase 1, a marker for AAMs has been found to be essential in both parasite expulsion
115 and wound healing during *H. polygyrus* infections (9,40). Collagen is a major component
116 of the ECM and excessive collagen deposition leads to fibrosis and scarring during
117 chronic helminth infections [41].
118
119 Immune responses are not only generated to tissue dwelling parasitic stages but also to
120 the adults found in the intestinal lumen. The cytokines IL-4 and IL-13 enhance smooth
121 muscle contractility of the intestine via STAT6 dependent pathways [42] to help
122 eliminate adult worms [43]–[45]. IL-4, IL-9 and IL-13 also regulate goblet cell hyperplasia
123 and increase mucus production during gastro-intestinal (GI) nematode infections
124 [46],[47], which makes it more difficult for adult parasites to coil around intestinal villi.
125 In addition, RELM-β produced by goblet cells interferes with the ability of adult parasites
126 to feed, thus limiting their numbers [48]. Finally, *H. polygyrus* infections induce

127 polyclonal and parasite specific serum antibody responses, which function to limit adult
128 female egg production [5],[23],[27],[28].
129
130 Most of the murine studies on helminth infection use a bolus model of infection (one
131 large dose), with some groups adopting a drug clearance model (bolus infection, drug
132 clearance, bolus infection) to simulate mass drug administration programs [7],[49].
133 However, under natural conditions, GI nematodes are ubiquitous in the environment
134 [50] and hosts are constantly coming into contact with them. While many hosts are
135 infected, few have life threatening levels of worms implying immune regulatory
136 mechanisms are at play [5]. Most hosts are unable to clear infection but can limit
137 excessively damaging worm burdens [13]. Hence, we (and others) have set up
138 experimental infection models using trickle infections to study parasite clearance of GI
139 nematodes in a more natural setting [18],[51]–[53]. We use multiple low doses of
140 larvae, given over a specific time period to achieve this.
141
142 *H. polygyrus* trickle infections in genetically resistant and susceptible strains of mice
143 reveal that the frequency of infection is an important determinant of parasite expulsion,
144 where frequently infected mice eliminate worms more rapidly than mice infected with
145 the same total number of larvae but in less frequent doses [53]. The aim of our study
146 was to identify the host protective immune mechanisms underlying these results.
147 Previous studies speculated that improved antibody and innate immune cell responses
148 to tissue dwelling parasites were key elements [18],[53]. We were able to reproduce the

149 data demonstrating that in susceptible mice, trickle infection results in reduced worm
150 burdens. However, we were also able to show that this reduction was associated with
151 increased levels of antibodies bound to tissue larvae and a specific gene expression
152 signature in the granulomas. All other correlates of Th2 immunity measured between
153 the bolus- and trickle-infected mice were similar including systemic Th2 cytokine
154 responses and antibody levels, as well as local physiological, mucosal and immunological
155 responses in the small intestine. Our results highlight the importance of the granuloma
156 in the host's ability to clear *H. polygyrus* and emphasise the need to study this key tissue
157 in more depth, rather than using correlates such as general intestinal or systemic
158 responses.
159

160 **MATERIALS AND METHODS**
161

162 *Mice, parasites and antigen*
163

164 Female and male C57Bl/6 mice aged 6-8 weeks (bred and maintained at the animal care
165 facility, Department of Biological Sciences, University of Calgary or University of
166 California, Riverside, USA) were used for all experiments. All animal experiments were
167 approved by the University of Calgary's Life and Environmental Sciences Animal Care
168 Committee (protocols AC17-0083 and AC17-0240) and the University of California,
169 Riverside's Institutional Animal Care and Use Committee
170 (https://or.ucr.edu/ori/committees/iacuc.aspx; protocol A-20180023). All protocols for

171 animal use and euthanasia were in accordance with either the Canadian Council for
172 Animal Care (Canada) or National Institutes of Health (USA) guidelines. Animal studies
173 are in accordance with the provisions established by the Animal Welfare Act and the
174 Public Health Services (PHS) Policy on the Humane Care and Use of Laboratory Animals.
175
176 Female BALB/c mice and Swiss Webster mice aged 6-8 weeks were purchased from
177 Charles River Laboratories (Senneville, Quebec). Infected mice were orally gavaged with
178 200 third stage *Heligmosomoides polygyrus* larvae (maintained in house, original stock
179 was a gift from Dr. Allen Shostak, University of Alberta, Canada) and euthanized at
180 either 7, 14, 21 or 28 days post initial infection. Mice were infected according to the
181 bolus or trickle infection regimes (Fig 1A, 1B & 8A). To avoid differences in counts during
182 the trickle infections, on day 0, two identical bolus solutions were made up (200
183 worms/100ul). One was used to infect the bolus infected mice and one was used for the
184 trickle infected mice and diluted as necessary according to the number of trickle doses.
185
186 *H. polygyrus* antigen was prepared by collecting live adult worms from 14-day infected
187 mice using modified Baerman's apparatus. Worms were washed multiple times and
188 homogenized in PBS using a glass homogenizer. The resulting solution was centrifuged
189 (13, 000 g, 10 minutes, 4^0C) and the supernatant filtered (0.2µm filter, Nalgene). The
190 protein concentration was calculated using the Bradford assay. The antigen was stored
191 at 15 mg/ml at -80^0C.
192

193 *Adult worm burden and granuloma number*

194

195 Small intestines of infected mice were harvested and opened longitudinally. The number
196 of adult worms present in the intestinal lumen and of granulomas present along the
197 length of the small intestine were counted using a dissection microscope.

198

199 *Transit time*

200

201 Gastrointestinal transit time was measured one day prior to euthanasia. Mice were fasted
202 for 6 hours and 200 µl of 5% Evans blue (Sigma) in 5% gum arabic (ACROS organics) was
203 orally gavaged using a ball tip 20 gauge 1.5'', 2.25mm curved animal feeding needle. Each
204 mouse was labelled, with the time of dye administration recorded. Mice were transferred
205 to clean empty cages and the time to pass the first blue fecal pellet was recorded.
206 Gastrointestinal transit time was calculated for each mouse.

207

208 *Cell isolation and in vitro re-stimulation assay*

209

210 MLN and SPL were mechanically dissociated into single cell suspensions. Cells were
211 counted using a Beckman-Coulter ViCell XR. MLN and SPL were cultured at 1 x 10^6
212 cells/ml for 48 hours in RPMI medium, 10% FCS, 1% L-glutamine, 1% penicillin/
213 streptomycin (supplemented RPMI 1640) in the presence of 10 µg/ ml *H. polygyrus*

antigen or 2 µg/ml concanavalin A (Sigma) at 37 ^{0}C with 5% CO_2. Supernatants were collected for cytokine measurements. Measurements for antigen specific production were not included in the analysis unless cytokine production was observed in the wells with concanavalin A stimulation.

Serum

Blood samples were collected using a terminal cardiac bleed. Blood was left to clot for 30 minutes and then centrifuged twice at 11, 000 g at 4^{o}C for 10 minutes. Serum was collected and used either fresh or stored at -80^{o}C.

Intestinal Tissue homogenates

Small intestines were opened longitudinally and washed with PBS to remove luminal content. The mucosal surface was identified under a dissecting microscope. The mucosal surface (with its mucus) was gently scraped using a glass slide. Scrapings were weighed, added to 500 µl lysis buffer (10 µM tris HCl, 0.025% sodium azide, 1% tween 80, 0.02% phenylmethylsulfonyl fluoride) with one complete protease inhibitor tablet (Roche diagnostics GmbH, Germany) and homogenized using a bead beater (40 seconds at speed 6 using the Fast-prep-24 bead beater, MP biomedical). The homogenate was centrifuged at 11, 000 g at 4^{o}C for one hour. Supernatants were collected and used fresh or stored at -80^{o}C.

236

237 *ELISAs*

238

239 Cytokines in serum and intestinal tissue homogenates were measured by ELISA
240 according to manufacturer's guidelines (R & D systems, DY404 (IL-4), DY413 (IL-13),
241 DY594 (IL-21). Total IgE (BD, 555248) and IgA (capture antibody, BD, 556969, detection
242 antibody, BD, 556978) levels were measured by ELISA according to manufacturer's
243 instructions.

244

245 Antigen specific antibody responses were also measured by ELISA. ELISA microplates
246 were coated with 10 µg/ml *H. polygyrus* antigen in carbonate buffer (0.1mM $NaHCO_3$,
247 pH 9.6), overnight at 4°C. Plates were blocked with 2% BSA in TBS/0.05% tween 20 for 2
248 hours at 37°C. Sera were diluted in TBS Tween and added to wells overnight at 4°C.
249 Antigen- specific IgG_1 was detected with HRP-conjugated corresponding detection
250 antibodies (anti-IgG_1 (BD, 553441) with TMB peroxidase substrate (T3405, Sigma). The
251 reaction was stopped using 1M H2SO4 solution and the colour change was read at
252 450nm.

253

254 *Antibody detection in the granuloma*

255

256 Consecutive formalin fixed paraffin embedded mouse small intestinal sections were
257 deparaffinized using two, five-minute xylene washes, rehydrated by washing in 95%

ethanol and 70% ethanol for 5 minutes. Slides were incubated in 2% sodium borohydride (VWR, BDH4604) in PBS for 40 minutes at RT to remove auto fluorescence. Antigens were retrieved using 2.5% trypsin (Thermo scientific, 15090046) in 0.1% HEPES buffer, incubated at 37 ^{0}C for 25 minutes. Blocking steps were performed following PBS washes. All samples were blocked with starting block (Thermo Scientific, 37578) for 1 hour at RT and rat/rabbit/goat serum for 30 minutes at RT. Following blocking steps, slides were incubated with rat anti-mouse IgG_1 (BD, 562026), IgE conjugated to FITC (BD, 553415) or rat anti-mouse IgA (BD, 559354) overnight at 4^{o}C. For IgG_{2c} staining, slides were incubated overnight at 4^{o}C with unconjugated rabbit anti-mouse IgG_{2c} antibody (Invitrogen, SA5-10221) followed by incubation with goat anti-rabbit IgG conjugated to Alexafluor488 (ImmunoResearch Laboratories, 111-545-003) for 2 hours at RT. Slides were washed in PBS for 15 minutes and mounted with Fluoroshield with DAPI (Sigma, F56057). Images were acquired using Thorlabs Tide whole-slide scanning microscope, x20 objective and analysed using Fijji 5.59.05 software.

Nanostring nCounter gene expression assay

Intestinal tissue from naïve mice or dissected pooled granulomas from infected mice were snap frozen in liquid nitrogen and RNA was isolated using phenol-chloroform extraction (TRIZOL, Sigma). RNA was quantified using a nanodrop and 50 ng was used for the Myeloid Innate Immunity V2 panel (NanoString) according to the manufacturer's guidelines. Gene expression analysis was conducted in R (1). Gene counts obtained via the nanostring

hybridization assay were normalized with NanostringNorm (2) using the negative control probes, positive control probes and housekeeping genes Eif2b4, Polr1b, and Edc3. Of the 20 housekeeping genes included in the assay Eif2b4, Polr1b, and Edc3 were the only ones found to have consistent expression among all samples in preliminary comparisons that used all 20 housekeeping genes for normalization. Therefore Eif2b4, Polr1b, and Edc3 were the only housekeeping genes used for normalization in subsequent analyses. The normalized counts were then compared using DESeq2 (3) to find differentially expressed genes in pairwise comparisons between treatment groups. A false discovery rate adjusted p-value cut off of 0.05 and a fold-change cutoff of 2 were used to identify genes that were differentially expressed in each pairwise comparison. The data discussed in this publication have been deposited in NCBI's Gene Expression Omnibus (4) and are accessible through GEO Series accession number GSExxx (number will be available upon acceptance).

Statistical analysis (except for nanostring results)

Mann-Whitney and Kruskal Wallis tests with Dunn’s multiple comparisons were used to assess differences between either two or more experimental groups using GraphPad Prism.

RESULTS

C57Bl/6 mice develop a resistant phenotype when infected using the trickle regimen

Two inbred strains of mice, C57Bl/6 (genetically susceptible) and BALB/c (genetically resistant) [13] were infected with *H. polygyrus* according to the bolus or trickle adult infection regimes (Fig. 1A & 1B). When given a bolus infection of 200 worms, BALB/c mice, being partially resistant to *H. polygyrus*, eliminated the majority of their worms by 14 days post-infection (mean worm burden of 53, SD +/- 30, Fig. 1C). Worm burdens declined over time until day 28 post infection, where the average number of worms per mouse was 8.5. SD +/- 13 (Fig. 1C). In contrast, C57Bl/6 mice being susceptible to *H. polygyrus* harboured high numbers of adult worms (an approximate mean value of 100 worms per mouse, Fig. 1D) in the intestinal lumen at all time points tested (Fig. 1D left). When infected according to the trickle protocol, infection dynamics in BALB/c mice were similar to those infected with the bolus regimen, whereby mice had low burdens at all time points post-infection, with near complete clearance by day 28 post-infection (Fig. 1C). However, C57Bl/6 mice infected according to the trickle protocol also eliminated most of the adult worms by 28 days post infection (mean worm burden 11, SD +/- 22, Fig. 1D). This mirrored the BALB/c mice results (Fig. 1C) but was in stark contrast to the results obtained for C57Bl/6 mice infected according to the bolus protocol despite similar worm burdens at day 14 post-infection (bolus: 129, SD +/- 38, trickle: 106, SD +/- 24, Fig. 1D). Administering *H. polygyrus*

larvae in low frequent doses to C57Bl/6 mice changed their susceptibility to infection (Fig. 1D).

Systemic IL-4 and IL-13 responses do not differ between bolus and trickle infected mice.

H. polygyrus clearance has been associated with a strong Th2 response, specifically increases in IL-4 and IL-13 cytokines [54]–[56]. As the Th2 immune response develops in response to *H. polygyrus*, MLN (mesenteric lymph nodes) and SPL (spleen) cell numbers increase [57]. Despite BALB/c mice having higher numbers of cells than C57Bl/6 mice at all time points in both organs, we found no differences between the trickle and bolus groups in either strain at any of the time points in either of the organs (Fig. 2A-D, left panel).

We measured the levels of the antigen-specific Th2 cytokine production (IL-4 and IL-13) in both the MLN and SPL as well as in the serum of mice by ELISA. Levels of cytokines measured in BALB/c mice were in general higher than in C57Bl/6 mice, as has previously been reported [13],[58],[59]. In BALB/c animals, levels were increased early and remained elevated over the course of infection for IL-4 in the MLN (increased from day 7, Fig. 2A middle panel) and the SPL (increased from day 14, Fig. 2C middle panel) and IL-13 in the MLN (increased from day 14 but decreased by day 28, Fig. 2A right panel) and SPL (increased from day 7, Fig. 2C right panel). In C57Bl/6 animals, levels were increased early but decreased by the later time points for IL-4 in the MLN (decreased from day 21, Fig. 2B

346 middle panel) and the SPL (decreased from day 21, Fig. 2D middle panel) and IL-13 in the
347 MLN (decreased by day 28, Fig. 2B right panel) and SPL (increased over the whole
348 infection, Fig. 2D right panel). Levels of IL-4 and IL-13 were undetectable in the serum, as
349 seen by others [60].
350
351 Taken together, we show that despite differences in cytokine levels according to mouse
352 strain, organ and post-infectious time-point, no differences were detected between bolus
353 and trickle infected mice in any of the conditions tested (Fig. 2).
354
355 ***Serum antibody levels do not differ between trickle and bolus infected mice.***
356
357 IgE and parasite specific IgG1 have both been shown to increase during primary and
358 secondary *H. polygyrus* infection [49]. IgG1 has been associated with parasite clearance
359 [5] while IgE is thought to reduce parasite fecundity [23]. We investigated changes in
360 serum antibody responses following bolus and trickle infections in both BALB/c and
361 C57Bl/6 mice over the course of infection.
362
363 Despite an increase in total serum IgE over the course of infection in both mouse strains
364 (BALB/c maximum levels on day 14 post infection with 559 ng/ml, SD +/- 94 compared to
365 naïve levels at 68 ng/ml, SD +/- 58 and C57Bl/6 maximum levels on day 21 post-infection
366 with 624 ng/ml, SD +/- 445 compared to naïve levels of 40 ng/ml, SD +/- 21), there was

no difference in levels between bolus- and trickle-infected groups at any post-infection time point (Fig. 3A & B).

We also measured an increase in parasite specific IgG1 over time, as has previously been reported [23]. In BALB/c mice, at both days 21 and 28 post-infection, titers were above $10^{\wedge 4}$ (Fig. 3C), while in C57Bl/6 mice, despite an increase in titers, these remained below $10^{\wedge 4}$ at all time points (Fig. 3D). However, again, no differences were observed between trickle and bolus infected animals in either strain, at any time point. Also, no detectable levels of *H. polygyrus* larval or adult parasite antigen specific IgE, IgG2c or IgA were observed in the serum of bolus- or trickle-infected mice at any post-infection time point.

Local physiological, mucosal and immunological responses in the small intestine are not responsible for the improved protection observed in trickle-infected C57Bl/6 mice

Worm infections result in physiological changes in the small intestine that have been linked to promoting worm expulsion. These include increased intestinal smooth muscle contractility [61], and therefore, decreased intestinal transit time, as well as increased mucus production. We found that transit time (as measured by the time to pass dyed gavaged material) was reduced in infected C57Bl/6 animals by day 7 post infection, in both trickle and bolus infected groups by approximately 20% (Fig. 4A, left panel). However, this decrease was only apparent in trickle infected animals by day 21 post-infection (approximate 12% difference between the trickle- and bolus-infected groups).

389 At day 28 post-infection, the difference between bolus- and trickle-infected groups
390 disappeared (approximate 3% difference between the trickle and bolus infected
391 groups). We also measured mucus production indirectly through intestinal tissue
392 weights. Infected mice had significantly higher intestinal tissue weights at 7 days
393 (approximately 1.5 times naïve weights in both trickle- and bolus-infected mice) and 21
394 days (approximately 2.5 times naïve weights in both trickle- and bolus-infected mice)
395 compared to naïve animals. Levels had returned to naive levels by 28 days post-infection
396 (Fig. 4A, right panel). There was no difference between the bolus- and trickle- infected
397 groups.
398
399 Next, we measured the levels of the Th2 cytokines IL-4 and IL-13 by ELISA in intestinal
400 tissue, since both these cytokines have been associated with stimulating increased
401 mucus production in the small intestine [62]. While levels of IL-13 were increased at day
402 21 and 28 post-infection, they were not different between the trickle- and bolus-
403 infected groups (naïve: mean level 125 pg/ml, SD +/- 141, day 21: bolus mean level 558
404 pg/ml, SD +/- 268, trickle mean level 309 pg/ml, SD +/- 231, day 28: bolus mean level
405 363 pg/ml, SD +/- 254, trickle mean level 366 pg/ml, SD +/- 216, Fig. 4B, right panel).
406 Intestinal IL-4 levels were not increased at any point (approximately 40pg/ml) apart
407 from at day 21, where they were significantly increased in the bolus-infected group (132
408 pg/ml, SD +/- 85) and different to the trickle-infected group. No levels of IL-5, IL-9 or IL-
409 10 were detectable in intestinal tissue from control or infected mice.
410

411 Mucosal IgA levels, regulated by the cytokine IL-21 [63], are also increased in the
412 presence of intestinal dwelling parasites [64]. We therefore measured IgA and IL-21
413 levels in the small intestine (Fig. 4C). Intestinal IgA levels did not differ between bolus-
414 or trickle-infected mice over the course of infection (Fig. 4C, right panel). Interestingly,
415 levels in both infection groups were similar to naïve levels (1292 pg/ml, SD +/- 924) at
416 day 7 and 21 post-infection, but decreased at day 28 post-infection (bolus: 832 pg/ml,
417 SD +/- 754; trickle: 555 pg/ml, SD +/- 93). Contrastingly, IL-21 levels were increased at
418 day 21 and 28 post-infection (from 98 pg/ml, SD +/- 84 in naïve animals to
419 approximately 950 pg/ml in infected animals, Fig. 4C, left panel). Like IgA levels, they
420 were not different between trickle- and bolus-infected animals.
421
422 In summary, at the level of the small intestine, very few differences were observed
423 between bolus- and trickle-infected animals, and these differences were not associated
424 with reduced worm burden.
425
426 ***Unlike bolus infection, trickle infection results in stable granuloma numbers over the***
427 ***course of infection in C56BL/6 mice.***
428
429 Since few differences were recorded between trickle- and bolus-infected mice in the
430 small intestine, we focused on the host/parasite interface, the intestinal granuloma.
431

Granulomas are a characteristic response to intestinal roundworms [14]. In response to *H. polygyrus*., they are round, opaque hard structures protruding from the small intestinal wall, easily identifiable and quantifiable using a dissection microscope (Fig. 5A). We measured these structures in both C56Bl/6 and BALB/c mice over the course of infection (days 7, 14 , 21 and 28 days post-infection). We found that, BALB/c mice, both trickle- and bolus-infected, had consistently high granuloma numbers over the first three time points (granuloma numbers >45, Fig. 5B). At day 28 post-infection, numbers dropped below this. In C57Bl/6 mice, a similar pattern was observed for the bolus-infected mice: at days 7 and 14, granuloma numbers were high, and >45, at days 21 and 28, granuloma numbers were reduced to ~17 (Fig. 5C). However, in trickle-infected C57Bl/6 mice, granulomas remained > 45 for the entire time course (Fig. 5C).

In C56BL/6 mice, granulomas from bolus and trickle- infected mice have different patterns of gene expression.

Since protective immune responses to *H. polygyrus* infection are thought to be localized in the granuloma (92), we isolated all granulomas along the small intestine of bolus- and trickle-infected C57Bl/6 mice at days 7 and 21 post-infection. To identify the granuloma transcriptional profiles, we extracted the mRNA and quantified transcript levels using the nanostring myeloid innate immunity V2 panel. For naïve mice that do not have any granulomas along their small intestine, we harvested intestinal tissue from similar areas to those harvested in infected mice.

454 Using principal component (PC) analysis, we found that infection is responsible for the
455 largest differences observed between the three groups (naïve, bolus-infected and
456 trickle-infected) at both post-infection time points. Naïve and infected groups clustered
457 distantly from each other, with infection explaining 62.1% of the variation (PC1) at day 7
458 post-infection and 90.5% of the variation (PC1) at day 21 (Fig. 6). Along the second
459 principal component, granulomas from day 21 (but not day 7) infected mice clustered
460 separately according to their infection mode (trickle or bolus, Fig. 6).
461
462 We found a number of genes that were differentially expressed between naïve
463 intestinal tissue (naive group) and granuloma tissue (infected groups trickle and/or
464 bolus) at day 7 and day 21 post-infection. At day 7, a total of 40 genes were upregulated
465 in infected (NvT and NvB) vs. naïve animals: 9 are involved in cell migration, 11 in
466 chemokine signalling, 6 in ECM and 5 in lymphocyte activation (Fig. 7A, Fig. S1). Over
467 half of the upregulated genes (57%, 23/40) were also found to be upregulated at day 21
468 post-infection. Many of the identified differentially expressed (DE) genes have already
469 been implicated in the immune response to helminths, such as *Retnla, Arg1, Chil3, Chil4*
470 and *Retlnb* [48],[65]. Fifteen of the 40 genes were highly upregulated (more than 16-
471 fold); they are mostly involved in chemokine signaling, likely attracting macrophages
472 and eosinophils to the granuloma. A total of 46 genes were downregulated in infected
473 vs. naïve animals (NvT and NvB) at day 7 post-infection: 9 involved in cytokine signaling,
474 11 in growth factors, 8 in ECM, 6 in metabolism and 9 in lymphocyte activation. Seven of
475 these genes (~15%) were also downregulated at day 21 post-infection. Twenty four of

476 the 46 genes were highly downregulated, and were associated with all functional
477 categories. At day 21 post-infection, 75 genes were upregulated in infected vs. naïve
478 (NvT and NvB) (Fig. 8A, Fig. S2): 12 involved in cell migration, 12 in chemokine signalling,
479 17 in ECM, 14 as growth factors, 10 in metabolism and 15 in lymphocyte activation.
480 Forty-one of these 75 genes were highly upregulated; these are involved in attracting
481 macrophages and eosinophils (e.g. *chil4, chil3, Serpine 1, ccl7, cxcl3, cxcr4*), as well as
482 ECM remodelling (e.g. *mmp12, col1a2, cma1, Arg1*). Twelve genes were downregulated
483 in infected vs. naïve (NvT and NvB): 2 involved in cytokine signalling, 2 in growth factors,
484 2 in pathogen response and 3 in metabolism. None were highly downregulated: the
485 most downregulated gene was *nos2* at ~7 times.
486
487 When looking at differentially expressed genes between trickle- and bolus-infected
488 animals, we also found differences at both time points (day 7 and day 21). At day 7 post-
489 infection, 10 genes were upregulated in trickle (vs. bolus) infected animals (Fig. 7A &
490 7B): 3 are TLR related, 3 are growth factors and 3 are involved in cytokine signalling. Of
491 the 10 DE genes, 6 are highly upregulated: *Selp, Tlr6, Bcl2, Tlr12, Flrt2, Il3ra* and one is
492 also upregulated at day 21: *ccl3*. At day 21 post-infection, 24 genes were upregulated in
493 trickle (vs. bolus, Fig. 8A & 8B): 4 are TLR related, 7 are growth factors and 8 are
494 involved in cytokine signaling. Of the 24 DE genes, 3 were highly upregulated: *Adamts4*
495 involved in ECM, *Osm* involved in cytokine production and *Ndc80* involved in cell
496 division. Twelve genes were upregulated in bolus (vs. trickle) at day 21 post-infection
497 compared to none at day 7. Three of these genes were growth factors and three

498 involved in cytokine signaling. No genes were highly upregulated, all were expressed
499 below 7-fold and were associated with many different functions. The three most highly
500 upregulated in the bolus infected animals *(cxcr3, cxcr4, ptgdr*) are involved in eosinophil
501 recruitment and Th1 immunity.
502
503 Despite having many genes commonly expressed between the granulomas of trickle-
504 and bolus-infected mice, different gene expression signatures were identified between
505 these two modes of infection. Of the genes previously associated with immune
506 responses to helminths, granulomas from day 21 trickle-infected animals had higher
507 levels of *Il13* (associated with worm expulsion [47],[54]), S100A8 and S100A9
508 (associated with neutrophil recruitment [66]), and *Retlnb* (associated with worm death
509 [48]), as well as *ccl3* and *cxcl5* (inflammatory chemokines) expression. Surprisingly, we
510 found no differences between the trickle and bolus infections in any genes linked to Fc
511 receptor signalling, despite the importance of antibody-mediated worm killing by
512 macrophages and/or eosinophils within granulomas [14].
513
514 ***IgG1 is the only antibody subtype to accumulate around encysted larvae in trickle***
515 ***infected C57Bl/6 mice.***
516
517 The ability to immobilize and/or kill parasitic worm larvae has been linked to antibody-
518 mediated binding by myeloid cells in the granuloma [14]. IgG1, IgG2c, IgE and IgA
519 antibody subtypes have all been linked to larval binding and/or damage to varying

520 degrees. Since we found no differences in the expression of Fc receptor signalling genes
521 within the granuloma between bolus and trickle-infected groups, we measured the
522 accumulation of IgG1, IgG2c, IgE and IgA antibodies using immunofluorescence, both
523 within the intestine and focusing on the host parasite interface within the granulomas
524 (Fig. 9-10). First, we found that high levels of IgG1 in the serum at day 21 post-infection
525 (Fig. 3D) correlated with the presence of IgG1 in granulomas in both bolus- and trickle-
526 infected mice (Fig. S3A). At day 7, where antigen specific serum IgG1 could not be
527 detected (Fig. 3D), IgG1 levels were minimal and/or absent (Fig. S3B).
528
529 To study the host/parasite interface, we set up a trickle (larvae) model (Fig. 9A), in
530 which granulomas containing larvae (acute granulomas) and granulomas where larvae
531 had either escaped or been killed (chronic granulomas) could be observed. Using this
532 model, we found a high concentration of IgG1 at the host parasite interface at both day
533 14 and day 21 (Fig. 9B) post-infection in acute granulomas. However, in both trickle and
534 bolus infected animals, levels of IgG1 were similar in chronic granulomas (Fig. 9C). We
535 could not detect any IgG2c, IgE or IgA within acute granulomas of trickle (larvae)
536 infected mice (Fig. 10A). This was despite observing IgG2c in intestinal tissue infected by
537 *C. rodentium* (Fig. S4), IgE in the lamina propria of infected mice (Fig. 10B) and IgA in the
538 lamina propria and Peyer's patches of infected mice (Fig. 10C).
539

Overall, our data show that bolus and trickle infection result in similar systemic and tissue-wide immune responses. However, granuloma formation is distinct between the two types of infection, and correlate with different resistant phenotypes.

DISCUSSION

The formation of granulomas around tissue encysted *H. polygyrus* worms has been associated with resistance to infection [13]. The innate cells of the granuloma are thought to damage/kill worms in conjunction with antibodies and complement components [18],[27],[28]. We and others [13],[67] have shown that resistant BALB/c mice have more granulomas (Fig. 5) as well as higher levels of Th2 cytokines (Fig. 2) and parasite specific antibodies (Fig. 3) compared to susceptible C57Bl/6 mice. These differences are thought to contribute to the BALB/c resistance phenotype.

Using our trickle model, we observed a resistance phenotype in the C57Bl/6 mice as opposed to the susceptible phenotype of bolus infected animals (Fig. 1). The improved immune response we observed is likely due to the continuous stimulation of the host immune system by multiple low doses of larvae resulting in a greater number of more effective granulomas (better responsive myeloid cells and the presence of IgG1 antibodies, Fig. 8 & 9) and ultimately fewer adult worms (Fig. 1). Unlike differences observed between resistant BALB/c and susceptible C57Bl/6 mice, we found no significant differences between the systemic (serum antibody and spleen/MLN cytokine response, Fig. 2 & 3) or tissue-wide (intestinal tissue physiological, cytokine and antibody responses, Fig. 4) immune responses of bolus and trickle infected C57Bl/6

562 mice. Only when studying the granulomas themselves, at the host parasite interface,
563 were important differences observed (Fig. 8 & 9).
564
565 Granulomas are made up of myeloid cells (mainly alternatively activated macrophages
566 and eosinophils) and $CD4^+$ T cells [7],[12] that accumulate around tissue encysted
567 worms and immobilize them. As expected [14], we identified increased gene expression
568 linked to myeloid cell recruitment, Th2 immunity and ECM deposition in granulomas
569 from both trickle and bolus infected groups, at both time points (Fig. 7 & 8).
570 Overall, the increased levels of myeloid cell chemotactic gene expression within
571 granulomas at day 7 in both bolus and trickle infections highlights the strong response
572 to the tissue dwelling phase of the parasite. Ten of the highly upregulated genes at day
573 7 post-infection (NvT and NvB) have been previously associated with immune responses
574 to helminth infections. And at day 21 post-infection, many of these same genes
575 remained upregulated, with an increase in the expression of genes related to ECM
576 remodelling (Fig. S1 & S2). Granulomas are novel structures created around tissue
577 dwelling worms. They are not observed in naïve animals (Fig. 5A). As such, we observed
578 the increased expression of genes associated with collagen production. At day 7 post-
579 infection, *col1a2* was upregulated with infection (NvT and NvB) as seen in other
580 helminth infections [68],[69]. At day 21 post-infection, *Col3a1, Col4a1 and Col15a1* were
581 also upregulated. This is the first time a direct involvement of type III, type IV and type
582 XV alpha 1 collagens have been linked to wound healing in an intestinal parasitic
583 infection.

584 In the bolus-infected mice at day 7 post-infection, a number of genes were
585 downregulated compared to trickle-infected animals (Fig. 7B). These genes are
586 associated with growth factors, as well as TLR and cytokine signalling, in dendritic cells.
587 This could be attributed to the initial parasite dose. Bolus-infected animals were given a
588 dose of 200 worms, known to strongly downregulate the immune response as early as
589 day 7 in the small intestine [70]. The trickle-infected animals received the same total
590 dose, but split over 3 different time points which may have reduced the impact of the
591 parasite. Interestingly, one of the downregulated genes on day 7 post-infection, *Bcl2*
592 (decreased by 33 fold compared to trickle-infected mice), has previously been
593 associated with *H. polygyrus* infection. It was found to be increased in CD4+ T cells in the
594 MLN, 2 weeks post-infection [71]. Similarly, we also found it was increased ~4 fold at
595 day 21 post-infection in the granulomas of both bolus- and trickle-infected animals (Fig.
596 S2).
597 At day 21, the two most highly expressed genes in the trickle-infected mice are involved
598 in tissue remodelling (*Adamts4*: 124 fold, *Osm*: 49 fold, [72]). *Adamts12* (7 fold increase,
599 (5)), *Adamts3* (6 fold increase, (6)), *Hdac5* (3 fold increase, [73]), *Smad2* (2 fold increase
600 [74]), and *Socs 3* (2 fold increase, [75]), were also upregulated and are involved in tissue
601 remodelling. The expression for all these genes is significantly higher compared to both
602 day 21 and day 7 bolus-infected mice. As such, the difference observed is not due to the
603 difference in 'age' of the granulomas, with the bolus day 21 granulomas being 'older'
604 than the trickle day 21 granulomas. Interestingly, to our knowledge, the 2 most highly
605 expressed genes (*Adamts4* and *Osm*) have not been associated with helminth infection

606 before. However, *Osm* is thought to stimulate *adamts4* mediated degradation of the
607 ECM [72], which may be an important process in the regulation of the granuloma
608 structure.
609
610 We also found genes involved in the Th2 response upregulated in the day 21 post-
611 infection trickle-infected animals. *Il-13* was increased 10-fold in the trickle- vs. bolus-
612 infected animals. While *Igf1* was increased 4-fold. Igf1 is secreted by alternatively
613 activated macrophages, and has been shown to promote worm expulsion. In
614 *Nippostrongylus brasiliensis* infected mice, animals lacking *Igf1* had higher worm counts
615 than their wildtype counterparts [76].
616
617 Granulomas from trickle-infected animals have a different transcriptomic signature to
618 bolus-infected animals, with a stronger Th2 and wound healing response. However,
619 worm killing depends not only on activated myeloid cells, but also antibodies.
620 Antibodies are thought to be the bridge that allows granuloma granulocytes to
621 kill/damage trapped parasites [14]. Antibodies are known to be required for protective
622 immunity against *H. polygyrus* as B cell deficient mice [80] and mice lacking antibody
623 production (J_H or AID deficient, [23]), fail to eliminate adult worms. Of all the antibody
624 isotypes, only IgG_1 from immune mice has been shown to reduce adult worm burdens
625 when administered alone [20], and protect mice from re-infection [22]. Passive transfer
626 of IgG_1 resulted in stunted worms, and *in vitro* assays demonstrated that IgG_1 promotes
627 peritoneal exudate cell attachment to the larval surface [20]. We found that IgG_1 was

628 the only detectable antibody isotype observed within the granulomas of infected mice
629 (Fig. 9 & 10). No IgE or IgA accumulation was detected (Fig. 10A), despite their presence
630 in the intestinal tissue (Fig. 10B & 10C), serum (Fig. 3B) and intestinal scrapings (Fig. 4C).
631 Interestingly, others have shown that while IgE was found to play no role in parasite
632 clearance in *H. polygyrus* infected animals, IgA contributes to limiting worm
633 development [23]. This was done using IgA deficient animals, and, unlike in our study,
634 levels of antibodies within granulomas were not assessed.
635
636 Trickle and bolus infected mice had similar levels of serum IgG_1 (Fig. 3) and of IgG_1
637 accumulation in their chronic granulomas (containing no tissue dwelling phases) at day
638 21 post-infection (SupFig. 3A). At this time point, tissue encysted worms had either
639 escaped or been killed and digested within the granulomas in both infected groups. To
640 detect whether IgG_1 was playing a role in damaging/killing incoming worms in the trickle
641 model (as has been suggested by [53]), we examined granulomas earlier (3/4 days as
642 opposed to 10 days) after the last trickle dose in order to observe tissue dwelling worms
643 within granulomas (Fig. 9A). In the granulomas containing worms, IgG_1 was
644 concentrated around the parasites (Fig. 8C). This observation helps explain how
645 antibodies play a role in worm clearance. Two weeks following infection, both bolus-
646 and trickle-infected mice produce a strong parasite specific IgG_1 response (high serum
647 titers, Fig. 3D). However, IgG_1 antibodies can only play a role in ADCC and direct parasite
648 killing/damage in trickle-infected mice when tissue encysted worms and IgG_1 are
649 present simultaneously in the granuloma. In bolus-infected animals, when high parasite

specific IgG_1 titers develop after two weeks of infection, larvae have already developed into adults and escaped from the granulomas into the intestinal lumen.

While the nanostring data obtained offer exciting new avenues of research into the regulation of granulomas, our study has some limitations. It is difficult to compare data from day 7 and day 21 post-infection with accuracy since they were obtained from mice of different sexes. Also, variation within groups was observed. Mouse 2 from the trickle group had much reduced gene expression than the other trickle-infected animals, which could in part be due to the low number of granulomas obtained from this animal. Finally, it would be interesting to study gene expression profiles of acute/chronic granulomas with/without tissue encysted worms from trickle/bolus infected mice using single cell RNA sequencing to provide new and valuable details at a cellular level. This would allow the differentiation of genes that are important during acute and chronic stages of infection, and help identify other mediators involved in antibody accumulation and ADCC as well as wound healing/fibrosis within the granulomas during infection.

ACKNOWLEDGEMENTS

We wish to thank Drs. Vuk Cerovic and Simon Hirota for insightful comments. This works was funded through Dr Finney's grants from the Canadian Foundation for Innovation and the Natural Sciences and Engineering Research Council of Canada (NSERC), Dr Nair's grant from the National Institutes of Health/NIAID (NIH R01AI153195) as well as scholarships for Drs Anupama Ariyaratne (NSERC Create in Host Parasite Interactions, UCalgary FGS

672 International Research Excellence Award and the Burroughs Wellcome Fund Travel
673 Award), Stephen Pollo (NSERC), Mayara Luzzi (Mitacs Globalink), Joel Bowron (NSERC),
674 Edina Szabo (UCalgary Eyes High).

675

677 **References**

678 1. **Johnston CJC, Robertson E, Harcus Y, Grainger JR, Coakley G, Smyth DJ, McSorley HJ,**
679 ***et al.*** Cultivation of Heligmosomoides polygyrus: an immunomodulatory nematode
680 parasite and its secreted products. *J. Vis. Exp.* 2015:e52412.DOI: 10.3791/52412.
681 2. **Reynolds L a.**, **Filbey KJ**, **Maizels RM**. Immunity to the model intestinal helminth
682 parasite Heligmosomoides polygyrus. *Semin. Immunopathol.* 2012; **34**:829–846.DOI:
683 10.1007/s00281-012-0347-3.
684 3. **Humphreys NE**, **Xu D**, **Hepworth MR**, **Liew FY**, **Grencis RK**. IL-33, a potent inducer of
685 adaptive immunity to intestinal nematodes. *J. Immunol.* 2008; **180**:2443–2449.DOI:
686 10.4049/jimmunol.180.4.2443.
687 4. **Muzio M, Bosisio D, Polentarutti N, D'amico G, Stoppacciaro A, Mancinelli R, van't**
688 **Veer C, *et al.*** Differential expression and regulation of toll-like receptors (TLR) in human
689 leukocytes: selective expression of TLR3 in dendritic cells. *J. Immunol.* 2000; **164**:5998–
690 6004.DOI: 10.4049/jimmunol.164.11.5998.
691 5. **Hewitson JP, Filbey KJ, Esser-von Bieren J, Camberis M, Schwartz C, Murray J,**
692 **Reynolds LA, *et al.*** Concerted activity of IgG1 antibodies and IL-4/IL-25-dependent
693 effector cells trap helminth larvae in the tissues following vaccination with defined
694 secreted antigens, providing sterile immunity to challenge infection. *PLoS Pathog.* 2015;
695 **11**:1–22.DOI: 10.1371/journal.ppat.1004676.
696 6. **Vella AT**, **Hulsebosch MD**, **Pearce EJ**. Schistosoma mansoni eggs induce antigen-
697 responsive CD44-hi T helper 2 cells and IL-4-secreting CD44-lo cells. Potential for T
698 helper 2 subset differentiation is evident at the precursor level. *J. Immunol.* 1992;

699 **14**:1714–1722.

700 7. **Anthony RM, Urban JF, Alem F, Hamed H a, Rozo CT, Boucher J-L, Van Rooijen N, *et***

701 ***al.*** Memory T(H)2 cells induce alternatively activated macrophages to mediate

702 protection against nematode parasites. *Nat. Med.* 2006; **12**:955–60.DOI:

703 10.1038/nm1451.

704 8. **Hewitson J, Murray J, Filbey K, Smith KA, Maizels RM, Hewitson JP, Murray J, *et al.***

705 Immune modulation and modulators in Heligmosomoides polygyrus infection. *Exp.*

706 *Parasitol.* 2011; **132**:76–89.DOI: 10.1016/j.exppara.2011.08.011.

707 9. **King IL**, **Mohrs K**, **Mohrs M**. A nonredundant role for IL-21 receptor signaling in

708 plasma cell differentiation and protective type 2 immunity against gastrointestinal

709 helminth infection. *J. Immunol.* 2010; **185**:6138–6145.DOI: 10.4049/jimmunol.1001703.

710 10. **Patnode ML**, **Bando JK**, **Krummel MF**, **Locksley RM**, **Rosen SD**. Leukotriene B 4

711 amplifies eosinophil accumulation in response to nematodes. *J. Exp. Med.* 2014;

712 **211**:1281–1288.DOI: 10.1084/jem.20132336.

713 11. **Pearce EJ**, **Macdonald AS**. The immunobiology of schistosomiasis. *Nat. Rev.*

714 *Immunol.* 2002; **2**:499–511.DOI: 10.1038/nri843.

715 12. **Morimoto M, Morimoto M, Xiao S, Anthony RM, Star RA, Urban JF, Gause C, *et al.***

716 Peripheral CD4 T cells rapidly accumulate at the host:parasite interface during an

717 inflammatory Th2 memory response. *J. Immunol.* 2004; **172**:2424–2430.DOI:

718 10.4049/jimmunol.172.4.2424.

719 13. **Filbey KJ, Grainger JR, Smith KA, Boon L, van Rooijen N, Harcus Y, Jenkins S, *et al.***

720 Innate and adaptive type 2 immune cell responses in genetically controlled resistance to

721 intestinal helminth infection. *Immunol. Cell Biol.* 2014; **92**:436–48.

722 14. **Ariyaratne A**, **Finney CAM**. Eosinophils and macrophages within the Th2-induced

723 granuloma: Balancing killing and healing in a tight space. *Infect. Immun.* 2019;

724 **87**:e00127-19.

725 15. **Wilson MS**, **Mentink-Kane MM**, **Pesce JT**, **Ramalingam TR**, **Thompson R**, **Wynn TA**.

726 Immunopathology of schistosomiasis. *Immunol. Cell Biol.* 2007; **85**:148–154.DOI:

727 10.1038/sj.icb.7100014.

728 16. **Hesse M, Modolell M, La Flamme AC, Schito M, Fuentes JM, Cheever AW, Pearce**

729 **EJ, *et al.*** Differential regulation of nitric oxide synthase-2 and arginase-1 by type 1/type

730 2 cytokines in vivo: granulomatous pathology is shaped by the pattern of L-arginine

731 metabolism. *J. Immunol.* 2001; **167**:6533–6544.

732 17. **Ben-Smith a.**, **Wahid FN**, **Lammas D a.**, **Behnke JM**. The relationship between

733 circulating and intestinal Heligmosomoides polygyrus-specific IgG1 and IgA and

734 resistance to primary infection. *Parasite Immunol.* 1999; **21**:383–395.DOI:

735 10.1046/j.1365-3024.1999.00236.x.

736 18. **Behnke JM**, **Lowe A**, **Clifford S**, **Wakelin D**. Cellular and serological responses in

737 resistant and susceptible mice exposed to repeated infection with Heligmosomoides

738 polygyrus bakeri. *Parasite Immunol.* 2003; **25**:333–340.DOI: 10.1046/j.1365-

739 3024.2003.00639.x.

740 19. **Dobson C**. Passive transfer of immunity with serum in mice infected with

741 Nematospiroides dubius: influence of quality and quantity of immune serum. *Int. J.*

742 *Parasitol.* 1982; **12**:207–213.DOI: 10.1016/0020-7519(82)90018-2.

743 20. **Pritchard DI**, **Williams DJ**, **Behnke JM**, **Lee TD**. The role of IgG1
744 hypergammaglobulinaemia in immunity to the gastrointestinal nematode
745 Nematospiroides dubius. The immunochemical purification, antigen-specificity and in
746 vivo anti-parasite effect of IgG1 from immune serum. *Immunology*. 1983; **49**:353–365.
747 21. **Pritchard DI**, **Behnke JM**, **Williams DJ**. Primary infection sera and IgG1 do not block
748 host-protective immunity to Nematospiroides dubius. *Immunology*. 1984; **51**:73–81.
749 22. **Williams DJ**, **Behnke JM**. Host protective antibodies and serum immunoglobulin
750 isotypes in mice chronically infected or repeatedly immunized with the nematode
751 parasite Nematospiroides dubius. *Immunology*. 1983; **48**:37–47.
752 23. **McCoy KD, Stoel M, Stettler R, Merky P, Fink K, Senn BM, Schaer C, *et al.*** Polyclonal
753 and Specific Antibodies Mediate Protective Immunity against Enteric Helminth Infection.
754 *Cell Host Microbe*. 2008; **4**:362–373. Available at:
755 https://linkinghub.elsevier.com/retrieve/pii/S1931312808002941.DOI:
756 10.1016/j.chom.2008.08.014.
757 24. **Ben-Smith A**, **Lammas DA**, **Behnke JM**. The relative involvement of Th1 and Th2
758 associated immune responses in the expulsion of a primary infection of
759 Heligmosomoides polygyrus in mice of differing response phenotype. *J. Helminthol.*
760 2003; **77**:133–146.DOI: 10.1079/JOH2003173.
761 25. **Wahid FN**, **Behnke JM**. Immunological relationships during primary infection with
762 Heligmosomoides polygyrus (Nematospiroides dubius): parasite specific IgG1 antibody
763 responses and primary response phenotype. *Parasite Immunol.* 1993; **15**:401–413.
764 26. **Wahid FN**, **Behnke JM**, **Grencis RK**, **Else KJ**, **Ben-Smith AW**. Immunological

765 relationships during primary infection with Heligmosomoides polygyrus: Th2 cytokines
766 and primary response phenotype. *Parasitology*. 1994; **108 (Pt 4**:461–471.DOI:
767 10.1017/s0031182000076022.
768 27. **Esser-von Bieren J, Mosconi I, Guiet R, Piersgilli A, Volpe B, Chen F, Gause WC, *et***
769 ***al.*** Antibodies trap tissue migrating helminth larvae and prevent tissue damage by
770 driving IL-4R-independent alternative differentiation of macrophages. *PLoS Pathog.*
771 2013; **9**:e1003771.DOI: 10.1371/journal.ppat.1003771.
772 28. **Esser-von Bieren J, Volpe B, Kulagin M, Sutherland DB, Guiet R, Seitz A, Marsland**
773 **BJ, *et al.*** Antibody-mediated trapping of helminth larvae requires CD11b and Fcγ
774 receptor I. *J. Immunol.* 2015; **194**:1154–1163.DOI: 10.4049/jimmunol.1401645.
775 29. **Song E**, **Ouyang N**, **Hörbelt M**, **Antus B**, **Wang M**, **Exton MS**. Influence of
776 alternatively and classically activated macrophages on fibrogenic activities of human
777 fibroblasts. *Cell. Immunol.* 2000; **204**:19–28.DOI:
778 https://doi.org/10.1006/cimm.2000.1687.
779 30. **Wynn T a**, **Ph D**, **Barron L**. Macrophages: master regulators of inflammation and
780 fibrosis. *Semin. Liver Dis.* 2010; **30**:245–257.DOI: 10.1055/s-0030-
781 1255354.Macrophages.
782 31. **Anthony B**, **Allen JT**, **Li YS**, **McManus DP**. Hepatic stellate cells and parasite-induced
783 liver fibrosis. *Parasit. Vectors*. 2010; **3**:60.DOI: 10.1186/1756-3305-3-60.
784 32. **Friedman SL**. Mechanisms of disease: mechanisms of hepatic fibrosis and
785 therapeutic implications. *Nat. Clin. Pract. Gastroenterol. &Amp; Hepatol.* 2004; **1**:98.
786 33. **Tomasek JJ**, **Gabbiani G**, **Hinz B**, **Chaponnier C**, **Brown RA**. Myofibroblasts and

787 mechano-regulation of connective tissue remodelling. *Nat. Rev. Mol. Cell Biol.* 2002;
788 **3**:349.
789 34. **Wynn TA**. Common and unique mechanisms regulate fibrosis in various
790 fibroproliferative diseases. *J. Clin. Invest.* 2007; **117**:524–529.DOI: 10.1172/JCI31487.
791 35. **Faz-López B**, **Morales-Montor J**, **Terrazas LI**. Role of macrophages in the repair
792 process during the tissue migrating and resident helminth infections. *Biomed Res. Int.*
793 2016; **2016**:8634603.DOI: 10.1155/2016/8634603.
794 36. **Chen G**, **Wang SH**, **Jang JC**, **Odegaard JI**, **Nair MG**. Comparison of RELM-alpha and
795 RELM-beta single- and double-gene- deficient mice reveals that RELM-alpha expression
796 dictates inflammation and worm expulsion in hookworm infection. *Infect. Immun.* 2016;
797 **84**:1100–1111.DOI: 10.1128/IAI.01479-15.Editor.
798 37. **Teng X**, **Li D**, **Champion HC**, **Johns RA**. FIZZ1/RELM-alpha, a novel hypoxia-induced
799 mitogenic factor in lung with vasoconstrictive and angiogenic properties. *Circ. Res.* 2003;
800 **2**:1065–1067.DOI: 10.1161/01.RES.0000073999.07698.33.
801 38. **Schultz G**, **Clark W**, **Rotatori DS**. EGF and TGF-α in wound healing and repair. *J. Cell.*
802 *Biochem.* 1991; **45**:346–352.DOI: 10.1002/jcb.240450407.
803 39. **Wong DTW, Donoff RB, Yang J, Song B-Z, Matossian K, Nagura N, Elovic A, *et al.***
804 Sequential expression of transforming growth factors α and β(1) by eosinophils during
805 cutaneous wound healing in the hamster. *Am. J. Pathol.* 1993; **143**:130–142.
806 40. **Herbert DBR, Holscher C, Mohrs M, Arendse B, Schwegmann A, Radwanska M,**
807 **Leeto M, *et al.*** Alternative macrophage activation is essential for survival during
808 schistosomiasis and downmodulates T Helper 1 responses and immunopathology.

Immunity. 2004; **20**:623–635.

41. **Wynn TA**. Cellular and molecular mechanisms of fibrosis. *J. Pathol.* 2008; **214**:199–210.DOI: 10.1002/path.2277.

42. **Zhao A, McDermott J, Urban JF, Gause W, Madden KB, Yeung KA, Morris SC, *et al.*** Dependence of IL-4, IL-13, and Nematode-Induced Alterations in Murine Small Intestinal Smooth Muscle Contractility on Stat6 and Enteric Nerves. *J. Immunol.* 2003; **171**:948 LP – 954.DOI: 10.4049/jimmunol.171.2.948.

43. **Vallance BA**, **Blennerhassett PA**, **Collins SM**. Increased intestinal muscle contractility and worm expulsion in nematode-infected mice. *Am. J. Physiol. Liver Physiol.* 1997; **272**:G321–G327.DOI: 10.1152/ajpgi.1997.272.2.G321.

44. **Marillier RG, Brombacher TM, Dewals B, Leeto M, Barkhuizen M, Govender D, Kellaway L, *et al.*** IL-4Rα-responsive smooth muscle cells increase intestinal hypercontractility and contribute to resistance during acute Schistosomiasis. *Am. J. Physiol. Liver Physiol.* 2010; **298**:G943–G951.DOI: 10.1152/ajpgi.00321.2009.

45. **Vallance BA**, **Blennerhassett PA**, **Deng Y**, **Matthaei KI**, **Young IG**, **Collins SM**. IL-5 contributes to worm expulsion and muscle hypercontractility in a primary T. spiralisinfection. *Am. J. Physiol. Liver Physiol.* 1999; **277**:G400–G408.DOI: 10.1152/ajpgi.1999.277.2.G400.

46. **Townsend JM**, **Fallon GP**, **Matthews JD**, **Smith P**, **Jolin EH**, **McKenzie NA**. IL-9-deficient mice establish fundamental roles for IL-9 in pulmonary mastocytosis and goblet cell hyperplasia but not T cell development. *Immunity*. 2000; **13**:573–583.DOI: 10.1016/s1074-7613(00)00056-x.

831 47. **Urban JFJ**, **Noben-Trauth N**, **Donaldson DD**, **Madden KB**, **Morris SC**, **Collins M**,
832 **Finkelman FD**. IL-13, IL-4Ralpha, and Stat6 are required for the expulsion of the
833 gastrointestinal nematode parasite Nippostrongylus brasiliensis. *Immunity*. 1998; **8**:255–
834 264.DOI: 10.1016/s1074-7613(00)80477-x.
835 48. **Herbert DR, Yang J-Q, Hogan SP, Groschwitz K, Khodoun M, Munitz A, Orekov T, *et***
836 ***al.*** Intestinal epithelial cell secretion of RELM-beta protects against gastrointestinal
837 worm infection. *J. Exp. Med.* 2009; **206**:2947–57.DOI: 10.1084/jem.20091268.
838 49. **Mccoy KD, Stoel M, Stettler R, Merky P, Fink K, Senn BM, Schaer C, *et al.*** Article
839 Polyclonal and Specific Antibodies Mediate Protective Immunity against Enteric
840 Helminth Infection. 2008:362–373.DOI: 10.1016/j.chom.2008.08.014.
841 50. **Basyoni MMA**, **Rizk EMA**. Nematodes ultrastructure: complex systems and
842 processes. *J. Parasit. Dis.* 2016; **40**:1130–1140.DOI: 10.1007/s12639-015-0707-8.
843 51. **Bancroft AJ**, **Else KJ**, **Humphreys NE**, **Grencis RK**. The effect of challenge and trickle
844 Trichuris muris infections on the polarisation of the immune response. *Int. J. Parasitol.*
845 2001; **31**:1627–1637.DOI: https://doi.org/10.1016/S0020-7519(01)00281-8.
846 52. **Mihi B**, **Meulder FVAN**, **Vancoppernolle S**, **Rinaldi M**, **Chiers K**, **Broeck WVANDEN**.
847 Analysis of the mucosal immune responses induced by single and trickle infections with
848 the bovine abomasal nematode Ostertagia ostertagi. 2014; **13**:150–156.DOI:
849 10.1111/pim.12094.
850 53. **Brailsford TJ**, **Behnke JM**. The dynamics of trickle infections with Heligmosomoides
851 polygyrus in syngeneic strains of mice. *Int. J. Parasitol.* 1992; **22**:351–359.
852 54. **McKenzie GJ**, **Fallon PG**, **Emson CL**, **Grencis RK**, **McKenzie ANJ**. Simultaneous

disruption of interleukin (IL)-4 and IL-13 defines individual roles in T helper cell type 2-mediated responses. *J. Exp. Med.* 1999; **189**:1565–1572. Available at: /pmc/articles/PMC2193635/?report=abstract [Accessed October 8, 2020].DOI: 10.1084/jem.189.10.1565.

55. **Urban JF**, **Noben-Trauth N**, **Donaldson DD**, **Madden KB**, **Morris SC**, **Collins M**, **Finkelman FD**. IL-13, IL-4Rα, and Stat6 are required for the expulsion of the gastrointestinal nematode parasite Nippostrongylus brasiliensis. *Immunity*. 1998; **8**:255–264. Available at: https://pubmed.ncbi.nlm.nih.gov/9492006/ [Accessed October 8, 2020].DOI: 10.1016/S1074-7613(00)80477-X.

56. **Oeser K**, **Schwartz C**, **Voehringer D**. Conditional IL-4/IL-13-deficient mice reveal a critical role of innate immune cells for protective immunity against gastrointestinal helminths. *Mucosal Immunol.* 2015; **8**:672–682. Available at: https://pubmed.ncbi.nlm.nih.gov/25336167/ [Accessed October 8, 2020].DOI: 10.1038/mi.2014.101.

57. **King IL, Mohrs K, Meli AP, Downey J, Lanthier P, Tzelepis F, Fritz JH, *et al.*** Intestinal helminth infection impacts the systemic distribution and function of the naïve lymphocyte pool. *Mucosal Immunol.* 2017; **10**:1160–1168.

58. **Bancroft AJ**, **Grencis RK**, **Else KJ**, **Devaney E**. Cytokine production in BALB/c mice immunized with radiation attenuated third stage larvae of the filarial nematode, Brugia pahangi. *J. Immunol.* 1993; **150**:1395 LP – 1402.

59. **Matthew L**, **Little MC**, **Barrett J**, **Else KJ**. Absence of CC Chemokine Ligand 2 Results in an Altered Th1/Th2 Cytokine Balance and Failure to Expel Trichuris muris Infection.

2019.DOI: 10.4049/jimmunol.170.9.4693.

60. **Reynolds LA**, **Maizels RM**. In the absence of TGF-β signaling in T cells, fewer CD103+ regulatory T cells develop, but exuberant IFN-γ production renders mice more susceptible to helminth infection. *J. Immunol.* 2012; **189**:1113–7.

61. **Shea-donohue T**, **Notari L**, **Stiltz J**, **Sun R**, **Madden KB**, **Urban Jr JF**, **Zhao A**. Role of enteric nerves in immune-mediated changes in protease-activated receptor 2 effects on gut function. *Neurogastroenterol. Motil.* 2010; **22**:1138-e291.DOI: 10.1111/j.1365-2982.2010.01557.x.

62. **Fallon PG, Jolin HE, Smith P, Emson CL, Townsend MJ, Fallon R, Smith P, *et al.*** IL-4 induces characteristic Th2 responses even in the combined absence of IL-5, IL-9, and IL-13. *Immunity*. 2002; **17**:7–17.DOI: 10.1016/S1074-7613(02)00332-1.

63. **Cao AT**, **Yao S**, **Gong B**, **Nurieva RI**, **Elson CO**, **Cong Y**. Interleukin (IL)-21 promotes intestinal IgA response to microbiota. *Mucosal Immunol.* 2015; **8**:1072–1082. Available at: https://pubmed.ncbi.nlm.nih.gov/25586558/ [Accessed October 8, 2020].DOI: 10.1038/mi.2014.134.

64. **Strandmark J**, **Steinfelder S**, **Berek C**, **Kühl AA**, **Rausch S**, **Hartmann S**. Eosinophils are required to suppress Th2 responses in Peyer's patches during intestinal infection by nematodes. *Mucosal Immunol.* 2016; **10**:1–12.DOI: 10.1038/mi.2016.93.

65. **Nair MG, Gallagher IJ, Taylor MD, Loke P, Coulson PS, Wilson R a, Maizels RM, *et al.*** Chitinase and Fizz family members are a generalized feature of nematode infection with selective upregulation of Ym1 and Fizz1 by antigen-presenting cells. *Infect. Immun.* 2005; **73**:385–394.DOI: 10.1128/IAI.73.1.385-394.2005.

66. **Frohberger SJ, Fercoq F, Neumann A-L, Surendar J, Stamminger W, Ehrens A, Karunakaran I, *et al.*** S100A8/S100A9 deficiency increases neutrophil activation and protective immune responses against invading infective L3 larvae of the filarial nematode Litomosoides sigmodontis Bennuru S, ed. *PLoS Negl. Trop. Dis.* 2020; **14**:e0008119. Available at: https://dx.plos.org/10.1371/journal.pntd.0008119 [Accessed October 8, 2020].DOI: 10.1371/journal.pntd.0008119.

67. **Finney CA**, **Taylor MD**, **Wilson MS**, **Maizels RM**. Expansion and activation of CD4+CD25+ regulatory T cells in Heligmosomoides polygyrus infection. *Eur. J. Immunol.* 2007; **37**:1874–1886.DOI: 10.1002/eji.200636751.

68. **Olds GR**, **Griffin A**, **Kresina TF**. Dynamics of collagen accumulation and polymorphism in murine Schistosoma japonicum. *Gastroenterology*. 1985; **89**:617–624.DOI: https://doi.org/10.1016/0016-5085(85)90459-7.

69. **Park MK**, **Kim H-J**, **Cho MK**, **Kang SA**, **Park SY**, **Jang SB**, **Yu HS**. Identification of a host collagen inducing factor from the excretory secretory proteins of Trichinella spiralis. *PLoS Negl. Trop. Dis.* 2018; **12**:e0006516.

70. **Mosconi I, Dubey LK, Volpe B, Esser-von Bieren J, Zaiss MM, Lebon L, Massacand JC, *et al.*** Parasite proximity drives the expansion of regulatory T cells in Peyer's patches following intestinal helminth infection. *Infect. Immun.* 2015; **83**:3657–3665.

71. **Donskow-Łysoniewska K**, **Brodaczewska K**, **Doligalska M**. Heligmosomoides polygyrus antigens inhibit the intrinsic pathway of apoptosis by overexpression of survivin and Bcl-2 protein in CD4 T cells. *Prion*. 2013; **7**:319–327. Available at: /pmc/articles/PMC3904318/?report=abstract [Accessed October 7, 2020].DOI:

10.4161/pri.25008.

72. **Durigova M**, **Troeberg L**, **Nagase H**, **Roughley PJ**, **Mort JS**. Involvement of ADAMTS5 and hyaluronidase in aggrecan degradation and release from OSM-stimulated cartilage. *Eur. Cell. Mater.* 2011; **21**:31–45. Available at: http://www.ncbi.nlm.nih.gov/pubmed/21225593 [Accessed October 7, 2020].DOI: 10.22203/ecm.v021a03.

73. **Urbich C, Rössig L, Kaluza D, Potente M, Boeckel JN, Knau A, Diehl F, *et al.*** HDAC5 is a repressor of angiogenesis and determines the angiogenic gene expression pattern of endothelial cells. *Blood*. 2009; **113**:5669–5679. Available at: http://ashpublications.org/blood/article-pdf/113/22/5669/1488982/zh802209005669.pdf [Accessed October 7, 2020].DOI: 10.1182/blood-2009-01-196485.

74. **Grainger JR, Smith KA, Hewitson JP, McSorley HJ, Harcus Y, Filbey KJ, Finney CAM, *et al.*** Helminth secretions induce de novo T cell Foxp3 expression and regulatory function through the TGF-β pathway. *J. Exp. Med.* 2010; **207**:2331–41.

75. **Zhu B-M**, **Ishida Y**, **Robinson GW**, **Pacher-Zavisin M**, **Yoshimura A**, **Murphy PM**, **Hennighausen L**. SOCS3 Negatively Regulates the gp130-STAT3 Pathway in Mouse Skin Wound Healing. *J. Invest. Dermatol.* 2008; **128**:1821–1829. Available at: www.jidonline.org [Accessed October 7, 2020].DOI: 10.1038/sj.jid.5701224.

76. **Spadaro O**, **Camell CD**, **Bosurgi L**, **Nguyen KY**, **Youm YH**, **Rothlin C V.**, **Dixit VD**. IGF1 Shapes Macrophage Activation in Response to Immunometabolic Challenge. *Cell Rep.* 2017; **19**:225–234. Available at:

941 http://dx.doi.org/10.1016/j.celrep.2017.03.046http://dx.doi.org/10.1016/j.celrep.2017.
942 03.046 [Accessed October 7, 2020].DOI: 10.1016/j.celrep.2017.03.046.
943 77. **Alavi M V, Mao M, Pawlikowski BT, Kvezereli M, Duncan JL, Libby RT, John SWM,**
944 ***et al.*** Col4a1 mutations cause progressive retinal neovascular defects and retinopathy.
945 *Sci. Rep.* 2016; **6**:18602.DOI: 10.1038/srep18602.
946 78. **Ponticos M, Holmes AM, Shi-wen X, Leoni P, Khan K, Rajkumar VS, Hoyles RK, *et al.***
947 Pivotal role of connective tissue growth factor in lung fibrosis: MAPK-dependent
948 transcriptional activation of type I collagen. *Arthritis Rheum.* 2009; **60**:2142–2155.DOI:
949 10.1002/art.24620.
950 79. **Jiang X, Wu M, Xu XIN, Zhang L, Huang Y, Xu Z, He K, *et al.*** COL12A1 , a novel
951 potential prognostic factor and therapeutic target in gastric cancer. 2019:3103–
952 3112.DOI: 10.3892/mmr.2019.10548.
953 80. **Liu Q, Kreider T, Bowdridge S, Liu Z, Song Y, Gaydo AG, Urban JFJ, *et al.*** B cells have
954 distinct roles in host protection against different nematode parasites. *J. Immunol.* 2010;
955 **184**:5213–5223.DOI: 10.4049/jimmunol.0902879.
956
957 **FIGURE LEGENDS**
958
959 ***Figure 1: The trickle infection model results in C57Bl/6 mice developing a resistant***
960 ***phenotype.***
961 6-8 week old female C57Bl/6 and BALB/c mice were infected with 200 *H. polygyrus*
962 according to the bolus and trickle infection regimes. Adult worms were counted in the

963 small intestine at each time point using a dissection microscope. (A) Bolus infection
964 regimen: mice are infected with 200 larvae on Day 0 (in grey). Worms develop in the tissue
965 from day 0 to day 7 post-infection (in black), when adults emerge into the lumen and
966 reside there for the duration of infection (in black). Worms are counted in the intestinal
967 lumen on day 14, 21, and 28 post-infection. (B) Trickle infection regime: mice are infected
968 with 200 larvae in total, but in multiple doses over the course of infection (in grey). For
969 mice euthanised on day 7 post-infection (in black), doses of 50 larvae are trickled on days
970 0, 1, 2 and 3 post-infection. This allows enough time for the last dose of larvae to enter
971 the tissue and start developing. For mice euthanised on day 14 (in black), doses of 67
972 larvae are trickled on days 0, 2 and 4 post-infection. For mice euthanised on day 21 (in
973 black), doses of 33 larvae are trickled on days 0, 2, 4, 6, 8 and 10 post-infection. For mice
974 euthanised on day 28 (in black), doses of 20 larvae are trickled on days 0, 2, 4, 6, 8, 10,
975 12, 14, 16 and 18 post-infection. In each case (14, 21 and 28), there is a 10-day window
976 after the final dose to allow parasites to fully develop into adults and migrate from the
977 intestinal tissue to the intestinal lumen. (C) Worm burdens in BALB/c mice (white mouse)
978 infected according to the bolus (black circles) and trickle (white circles) regimes. (D) Worm
979 burdens in C57Bl/6 mice (black mouse) infected according to the bolus (black circles) and
980 trickle (white circles) regimens. For (C) and (D), graphs represent pooled data from 2
981 experiments, bars represent the median, with a minimum of 3 mice per group per
982 experiment. A Kruskal Wallis test with Dunn's multiple comparisons test was performed
983 to test for statistical significance between trickle and bolus groups at each time point, n.s.
984 = not significant, * = $p<0.05$.

985 ***Figure 2: Systemic IL-4 and IL-13 responses do not differ between bolus and trickle***
986 ***infected mice.*** 6-8 week old female C57Bl/6 and BALB/c mice were infected with 200 *H.*
987 *polygyrus* larvae according to the bolus and trickle infection regimes. Single cell
988 suspensions were isolated from the mesenteric lymph nodes and spleens; these were
989 cultured for 48 hours in the presence of *H. polygyrus* antigen. IL-4 and IL-13 cytokine levels
990 were measured in the supernatant by ELISA. (A) Viable cell numbers (left) with their IL-4
991 (middle) and IL-13 (right) production over the course of infection (d0, 7, 14, 21 and 28
992 post-infection) in the MLN of BALB/c (white) (A) and C57Bl/6 (black) mice (B) as well as
993 the SPL of BALB/c (white) (C) and C57Bl/6 (black) mice (D). Graphs represent pooled data
994 from 2 experiments, bars represent the median, with a minimum of 3 mice per group per
995 experiment. A Kruskal Wallis test with Dunn's multiple comparisons test was performed
996 to test for statistical significance between trickle (white circles) and bolus groups (black
997 circles) at each time point. No differences were found at any time point, in either organ,
998 in either strain.
999
1000 ***Figure 3: Serum IgG1 and IgE antibody levels do not differ between bolus and trickle***
1001 ***infected mice.*** 6-8 week old female C57Bl/6 (black) and BALB/c (white) mice were infected
1002 with 200 *H. polygyrus* larvae according to the bolus and trickle infection regimes. Serum
1003 antibody levels were measured by ELISA for total IgE in Balb/C (A) and C57Bl/6 (B) mice
1004 and parasite specific IgG1 for BALB/c (C) and C57Bl/6 (D) mice on days 0, 7, 14, 21 and 28
1005 post infection. Levels in naïve controls and at day 7 post-infection were undetectable for
1006 parasite specific IgG1. Graphs represent pooled data from 2 experiments, bars represent

1007 the median, with a minimum of 3 mice per group per experiment. A Kruskal Wallis test
1008 with Dunn's multiple comparisons test was performed to test for statistical significance
1009 between trickle (white circles) and bolus groups (black circles) at each time point. No
1010 differences were found at any time point, for either antibody, in either strain.
1011
1012 ***Figure 4: Aspects of the intestinal response to H. polygyrus differ between bolus and***
1013 ***trickle infected C57BL/6 mice at day 21 post-infection.*** 6-8 week old female C57Bl/6 mice
1014 were infected with 200 *H. polygyrus* larvae according to the bolus and trickle infection
1015 regimes and euthanised on days 7, 21 and 28 post-infection. (A) Mice were fasted for 6
1016 hours followed by Evans Blue administration. Time from dye administration to the passing
1017 of dyed fecal pellets was measured and normalised to control animals (left). Small
1018 intestines were dissected out and scraped using a glass slide leaving only the serosa. The
1019 intestinal scrapings were weighed for each mouse and normalised to control animals
1020 (right). (B) IL-4 (left) and IL-13 (right), as well as (C) IL-21 (left) and total IgA (right) were
1021 measured in the intestinal scrapings by ELISA. Graphs represent pooled data from a
1022 minimum of 2 experiments, bars represent the median, with a minimum of 2 mice per
1023 group per experiment. A Kruskal Wallis test with Dunn's multiple comparisons test was
1024 performed to test for statistical significance between trickle (white circles) and bolus
1025 (black circles) groups at each time point, n.s. = not significant, * = $p<0.05$.
1026
1027 ***Figure 5: Granuloma numbers remain stable over time in trickle-infected C56BL/6 mice.***
1028 6-8 week old female C57Bl/6 (black) and BALB/c (white) mice were infected with 200 *H.*

polygyrus according to the bolus and trickle infection regimes. Granuloma were counted in the small intestine at each time point using a dissection microscope. (A) Representative images of a portion of a naïve (left), a bolus (middle) and a trickle (left) infected small intestine at day 14 post-infection in C57Bl/6 mice. White arrows point to granulomas. Granuloma number in BALB/c (B) and C57Bl/6 (C) mice infected according to the bolus (black circles) and trickle (white circles) regimes. For (C) and (D), graphs represent pooled data from 2 experiments, bars represent the median, with a minimum of 3 mice per group per experiment. A Kruskal Wallis test with Dunn's multiple comparisons test was performed to test for statistical significance between trickle and bolus groups at each time point, n.s. = not significant, * = $p<0.05$, **** = $p<0.0001$.

Figure 6: Transcriptional profiles differ between granulomas from bolus and trickle infected mice. 6-8 week old female (7 days post-infection) and male (21 days post-infection) C57Bl/6 mice were infected with 200 *H. polygyrus* according to the bolus and trickle infection regimes. We used the nanostring nCounter mouse myeloid innate immunity V2 panel to measure the expression profiles of 754 gene encoding mRNAs within the granulomas. PCA plots highlighting differential gene expression at days 7 (left) and 21 (right) post infection.

Figure 7: Ten genes are differentially expressed between granulomas from bolus and trickle infected mice 7 days post-infection. . 6-8 week old female (7 days post-infection) C57Bl/6 mice were infected with 200 *H. polygyrus* according to the bolus and trickle

infection regimes. We used the nanostring nCounter mouse myeloid innate immunity V2 panel to measure the expression profiles of 754 gene encoding mRNAs within the granulomas. (A) Summary of differentially expressed genes (*adjusted p* < 0.05; FC >2) in each pairwise comparison showing differentially expressed genes in red and blue in a volcano plot, the total number of differentially expressed genes in the middle of the bidirectional arrows, and arrowheads showing the direction of differential expression for all and highly (FC = 4–16) differentially expressed genes. (B) Heatmap showing the relative expression of differentially expressed genes associated with the regulation of myeloid immune responses between bolus- and trickle-infected mice.

Figure 8: Thirty six genes are differentially expressed between granulomas from bolus and trickle infected mice 21 days post-infection. 6-8 week old male (21 days post-infection) C57Bl/6 mice were infected with 200 *H. polygyrus* according to the bolus and trickle infection regimes. We used the nanostring nCounter mouse myeloid innate immunity V2 panel to measure the expression profiles of 754 gene encoding mRNAs within the granulomas. (A) Summary of differentially expressed genes (*adjusted p* < 0.05; FC >2) in each pairwise comparison showing differentially expressed genes in red and blue in a volcano plot, the total number of differentially expressed genes in the middle of the bidirectional arrows, and arrowheads showing the direction of differential expression for all and highly (FC = 4–16) differentially expressed genes. (B) Heatmap showing the relative expression of differentially expressed genes associated with the regulation of myeloid immune responses between bolus- and trickle- infected mice.

1073 ***Figure 9: IgG1 antibodies accumulate around encysted larvae in the acute granulomas***
1074 ***of trickle-infected C57Bl/6 mice.*** 6-8 week old female C57Bl/6 mice were infected with
1075 200 *H. polygyrus* according to bolus and/or trickle models of infection. (A) Trickle infection
1076 regimen (acute granulomas): mice are infected with 200 larvae in total but spread out
1077 over infection (in grey). For mice euthanised on day 14 (in black), doses of 33 larvae are
1078 trickled on days 0, 2, 4, 6, 8 and 10 post-infection. For mice euthanised on day 21 (in
1079 black), doses of 20 larvae are trickled on days 0, 2, 4, 6, 8, 10, 12, 14, 16 and 18 post-
1080 infection. In each case (14 and 21), there is a 3-4 days window after the final dose to allow
1081 parasites to start developing in the mucosa and observe the formation of granulomas
1082 around them. (B & C) Formalin fixed, paraffin-embedded 6 µm sections were obtained
1083 from small intestine swiss rolls. These sections were co-stained with anti-mouse IgG1 and
1084 DAPI. Whole sections were studied using the Thorlabs Tide whole-slide scanning
1085 microscope, (20x objective). Antibody stain (left), isotype control stain (middle), and DAPI
1086 stain (right). (B) Representative acute granulomas (with worms, white dashed lines) from
1087 trickle nfected mice at 14 (top) and 21 (bottom) days post-infection. (C) Representative
1088 chronic granulomas (without worms, white dashed lines) from bolus (top) and trickle
1089 (bottom) infected mice at 21 days post-infection. Experiments were performed at least
1090 twice (minimum of 5 mice per group) and are representative of a total of 21 (bolus, day
1091 14 post-infection), 19 (of which 3 were acute granulomas, trickle, day 14 post-infection),
1092 7 (bolus, day 21 post-infection), 30 (of which 4 were acute granulomas, trickle, day 21
1093 post-infection) granulomas. Scale bar=100µm.
1094

Figure 10: IgG2c, IgE and IgA are not detected around encysted larvae in the granulomas of trickle infected mice. 6-8 week old female C57Bl/6 mice were infected with 200 *H. polygyrus* according to the trickle (larvae) model of infection. (A-C) Formalin fixed, paraffin-embedded 6 µm sections were obtained from small intestine swiss rolls. These sections were co-stained with antibodies to the IgG2c, IgE and/or IgA antibody subtype, as well as DAPI. Whole sections were studied using the Thorlabs Tide whole-slide scanning microscope, (20x objective). Experiments were performed once (minimum of 5 mice per group). Scale bar=100µm. (A) Representative images of granulomas from trickle infected mice at 21 days post-infection stained with either anti-mouse IgG2c (top), IgE (middle) or IgA (bottom). Antibody stain (left), DAPI stain (middle) and isotype control stain (right). Photographs are representative of a total of 15 granulomas (of which 3 were acute granulomas). The photographs here are of consecutive slides of the same granuloma as depicted in Fig. 8C, bottom. (B) Representative images of intestinal tissue from trickle-infected mice at 21 days post-infection stained with IgE. Antibody stain (left), DAPI stain (middle) and isotype control stain (right). White arrows point to IgE accumulation in the intestinal tissue. (D) Representative Peyer's Partch (top) and intestinal tissue (bottom) from trickle- infected mice at 21 days post-infection stained with IgA. Antibody stain (left), DAPI stain (middle) and isotype control stain (right). White arrows point to IgA accumulation in the intestinal villi (top) and Peyer's patches (bottom).

1117 ***Figure S1: Eighty six genes are differentially expressed between granulomas from naïve***
1118 ***and infected mice (NvT and NvB) 7 days post-infection.*** 6-8 week old female (7 days post-
1119 infection) C57Bl/6 mice were infected with 200 *H. polygyrus* according to the bolus and
1120 trickle infection regimes. We used the nanostring nCounter mouse myeloid innate
1121 immunity V2 panel to measure the expression profiles of 754 gene encoding mRNAs
1122 within the granulomas. Heatmap showing the relative expression of differentially
1123 expressed genes associated with the regulation of myeloid immune responses between
1124 naïve and infected mice (bolus and trickle).
1125
1126 ***Figure S2: Eighty eight genes are differentially expressed between granulomas from***
1127 ***naïve and infected mice (NvT and NvB) 21 days post-infection.*** 6-8 week old male (21
1128 days post-infection) C57Bl/6 mice were infected with 200 *H. polygyrus* according to the
1129 bolus and trickle infection regimes. We used the nanostring nCounter mouse myeloid
1130 innate immunity V2 panel to measure the expression profiles of 754 gene encoding
1131 mRNAs within the granulomas. Heatmap showing the relative expression of differentially
1132 expressed genes associated with the regulation of myeloid immune responses between
1133 naïve and infected mice (bolus and trickle).
1134
1135 ***Figure S3: IgG1 antibodies are present in the chronic granulomas of both bolus- and***
1136 ***trickle-infected mice at day 21 post-infection.*** 6-8 week old female C57Bl/6 mice were
1137 infected with 200 *H. polygyrus* according to bolus and/or trickle regimes. Formalin fixed,
1138 paraffin-embedded 6 µm sections were obtained from small intestine swiss rolls. These

sections were co-stained with anti-mouse IgG1 and DAPI. Whole sections were studied using the Thorlabs Tide whole-slide scanning microscope, (20x objective). Representative granulomas (white dashed line) from bolus- (top) and trickle- (bottom) infected mice at 21 days (A) and 7 days (B) post-infection. Antibody stain (left), isotype control stain (middle), and DAPI stain (right). For both groups, at day 7 post-infection, granulomas contained worms (acute granulomas) while at 21 days post-infection they did not (chronic granulomas). Experiments were performed at least twice (minimum of 5 mice per group) and are representative of a total of 5 (bolus, day 21 post-infection), 8 (trickle, day 21 post-infection), 8 (bolus, day 7 post-infection), and17 (trickle, day 7 post-infection), granulomas. Scale bar=100µm.

Figure S4: IgG2c is detectable in the intestinal tissue of C. rodentium infected mice. 6-8 week old female C57Bl/6 mice were infected with 5 x 10^8 cfu/ mouse *C. rodentium DBS100 strain* by gavage as a positive control for IgG2c staining. Formalin fixed, paraffin-embedded 6 µm sections were obtained from small intestinal swiss rolls. These sections were co-stained with antibodies to the IgG2c (left) as well as DAPI (right). Whole sections were visualized using the Thorlabs Tide whole-slide scanning microscope, (20x objective). Experiment was performed once (minimum of 5 mice per group). White arrows point to IgG2c staining within the lamina propria. Scale bar=100µm.

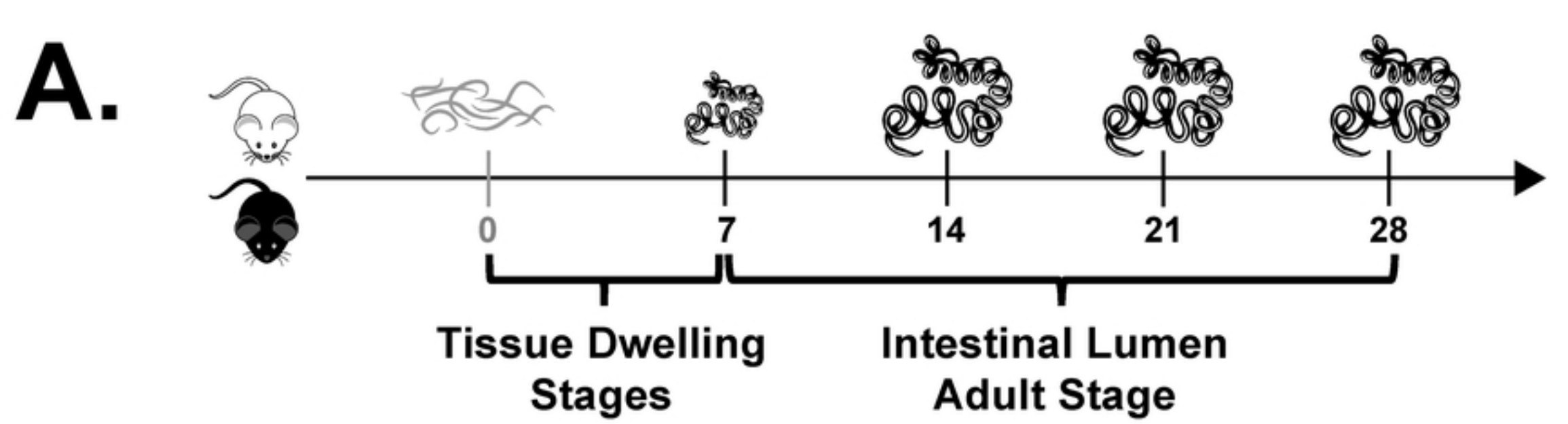

Figure 1

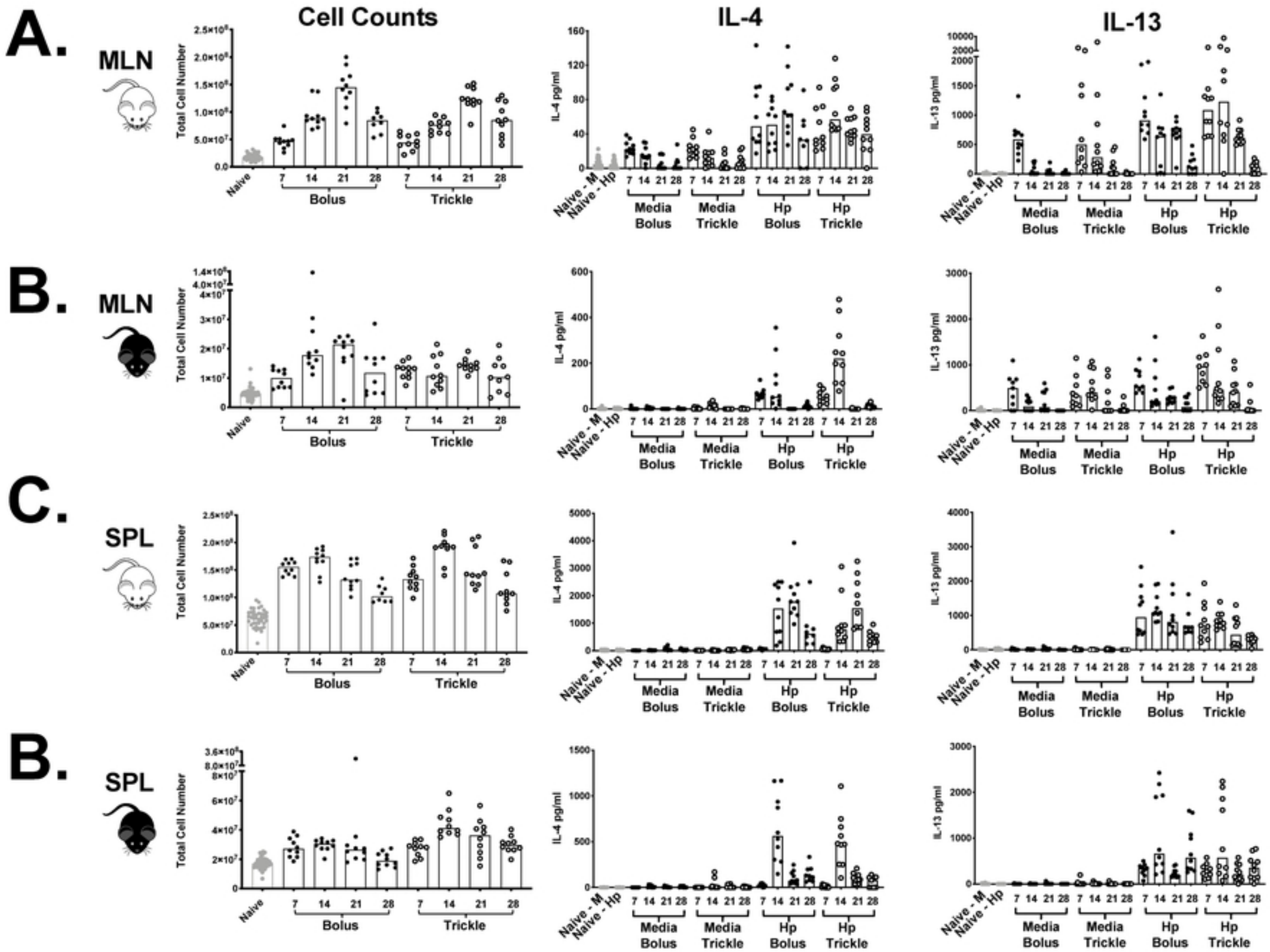
A.
MLN
Cell Counts
IL-4
IL-13
B.
MLN
C.
SPL
B.
SPL
Total Cell Number
IL-4 pg/ml
IL-13 pg/ml
Naive
Bolus
Trickle
Naive - M
Naive - Hp
Media Bolus
Media Trickle
Hp Bolus
Hp Trickle

Figure 2

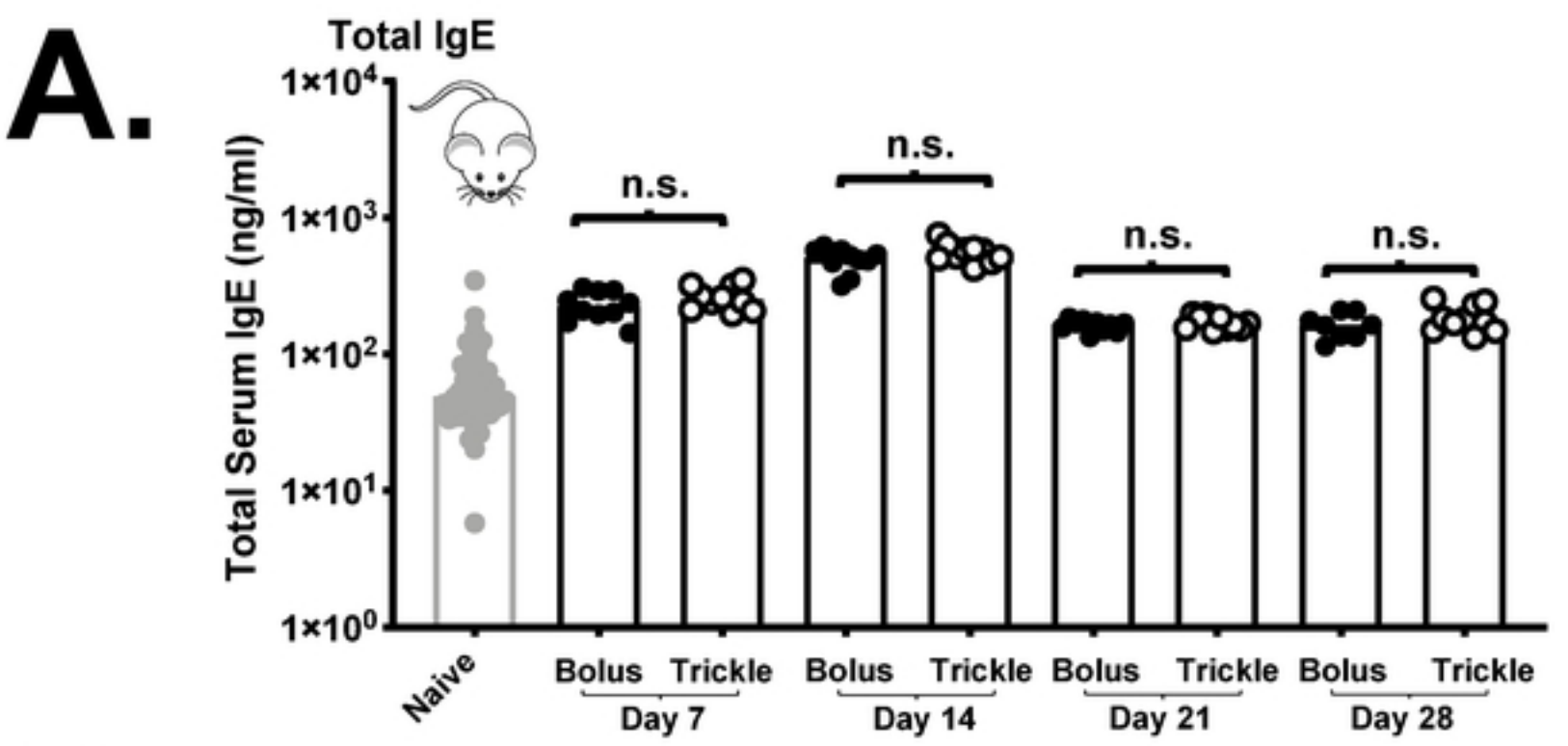

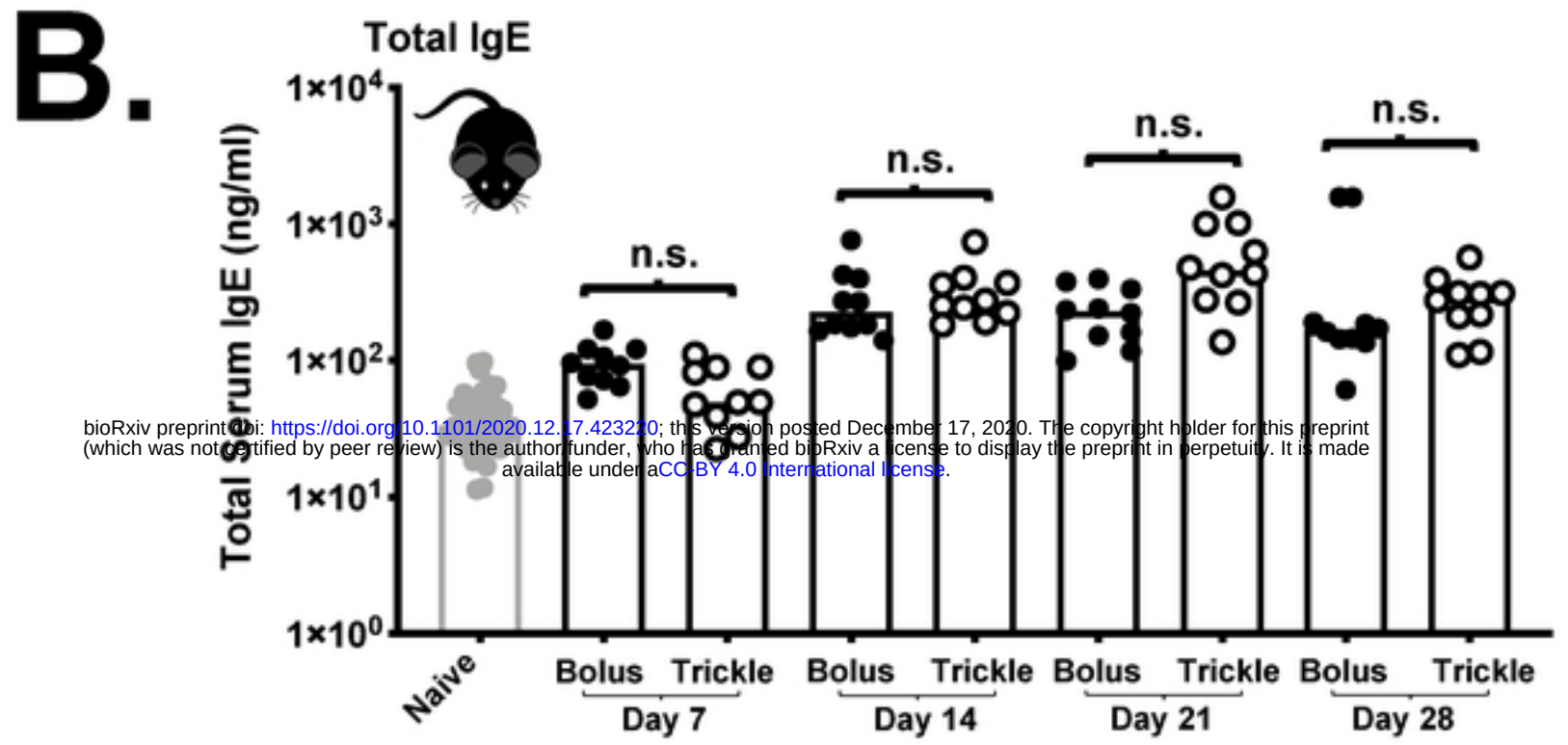

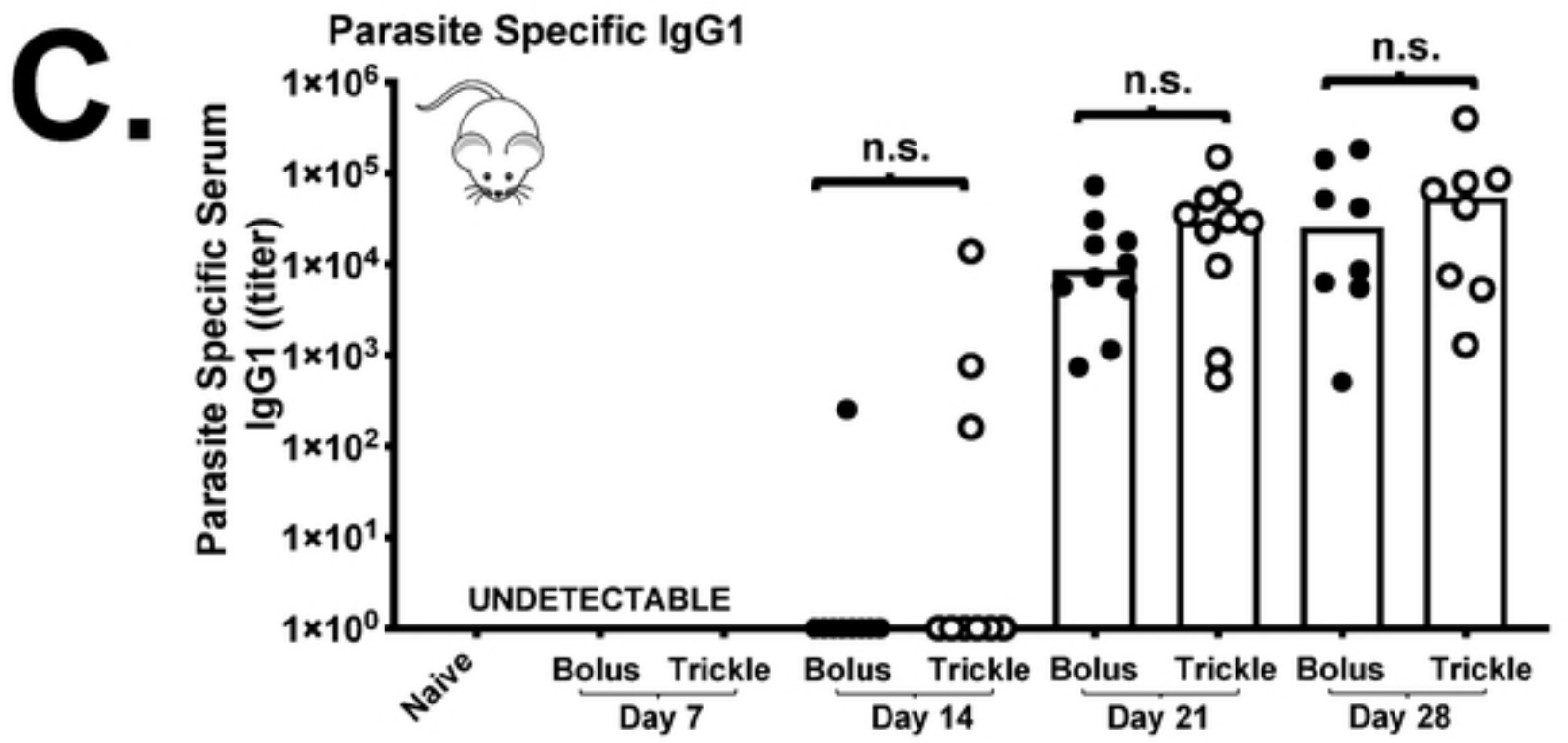

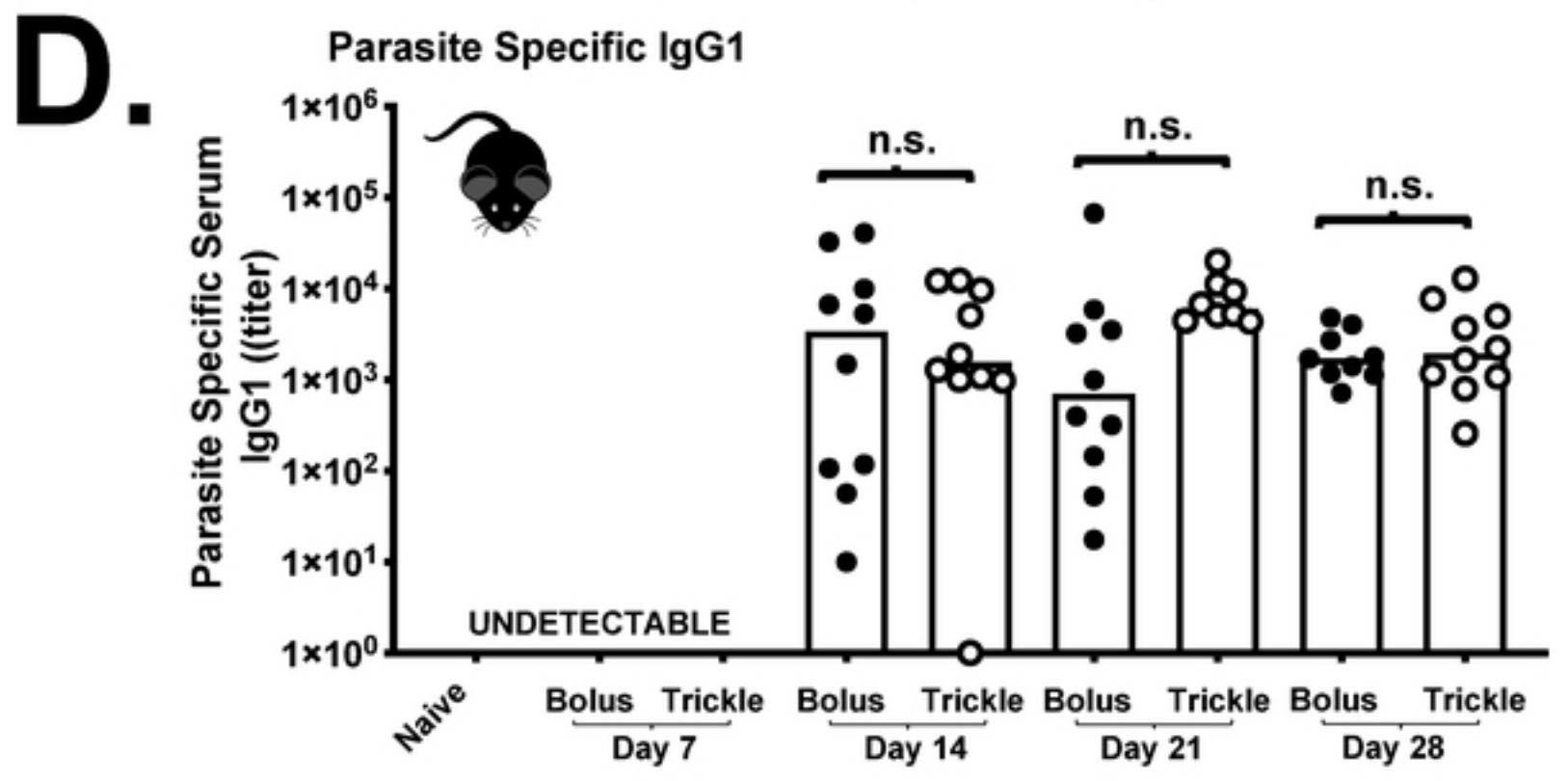

Figure 3

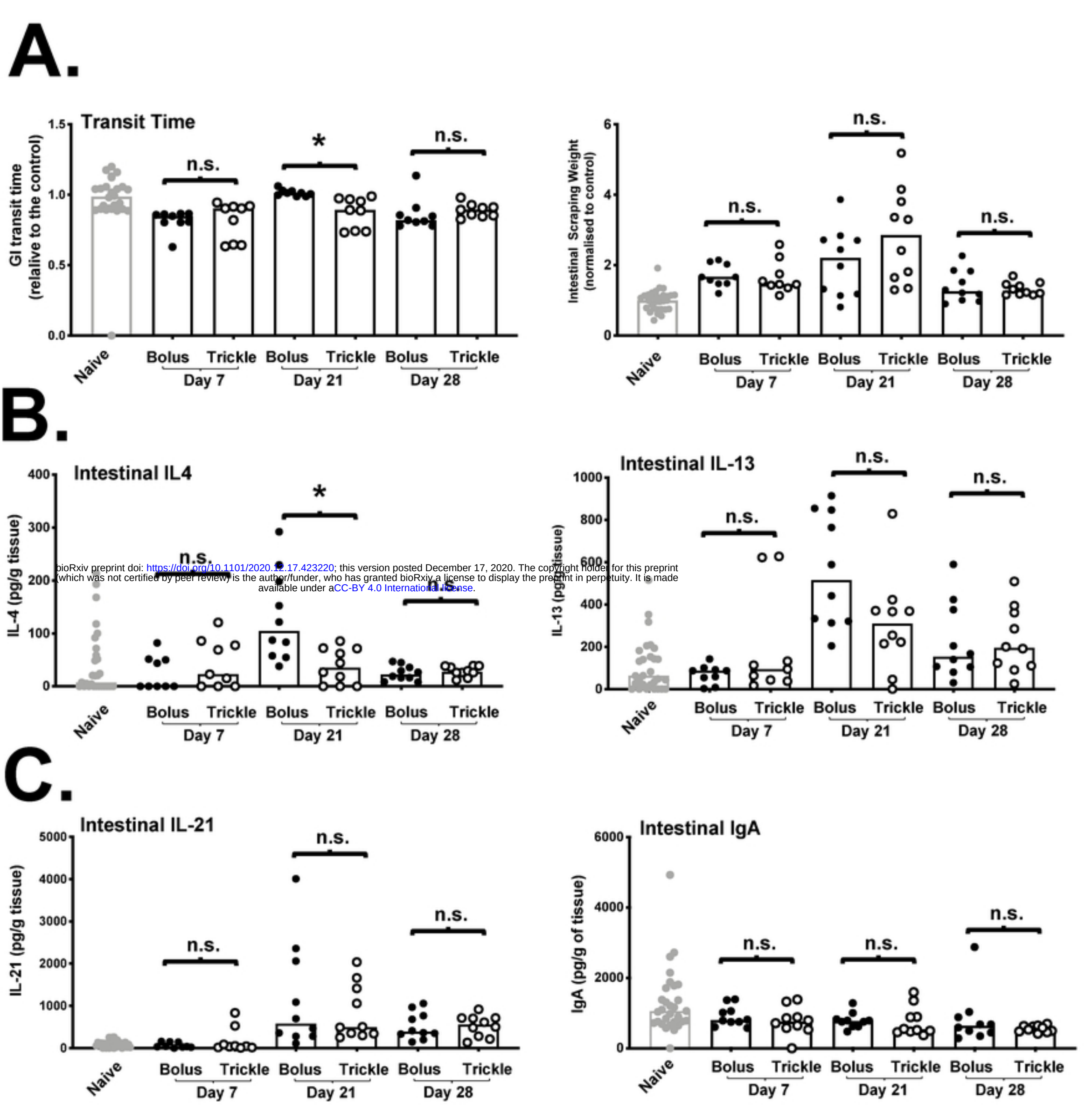

Figure 4

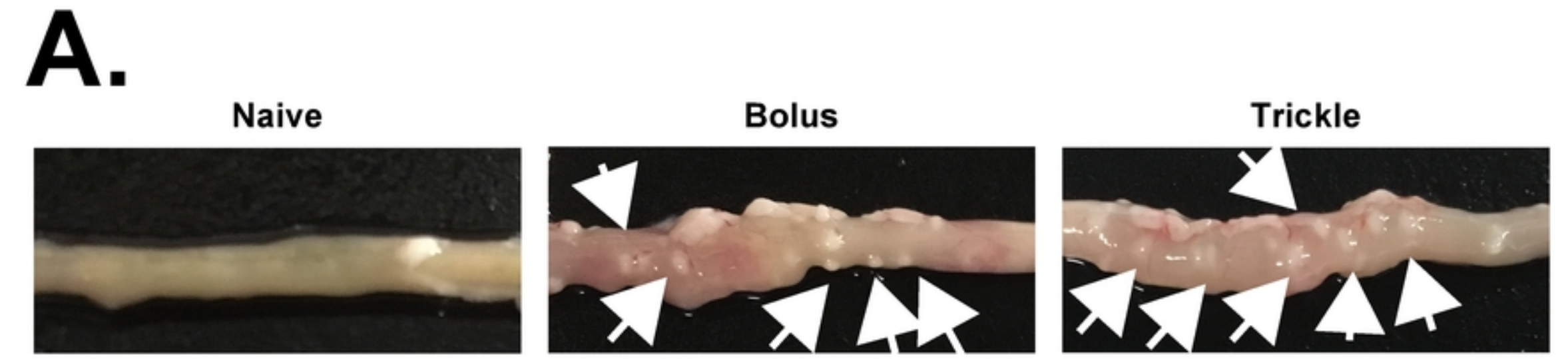

Figure 5

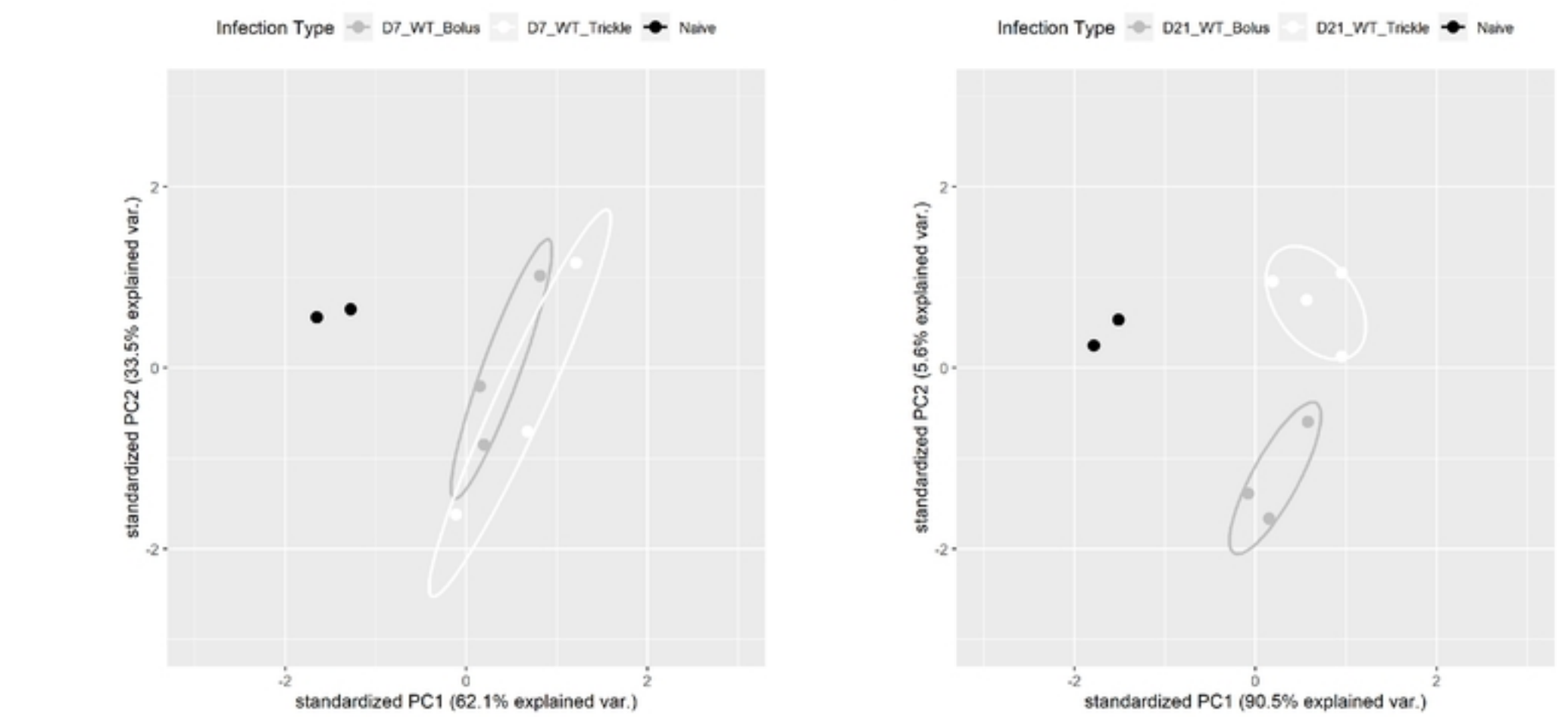

Figure 6

A.

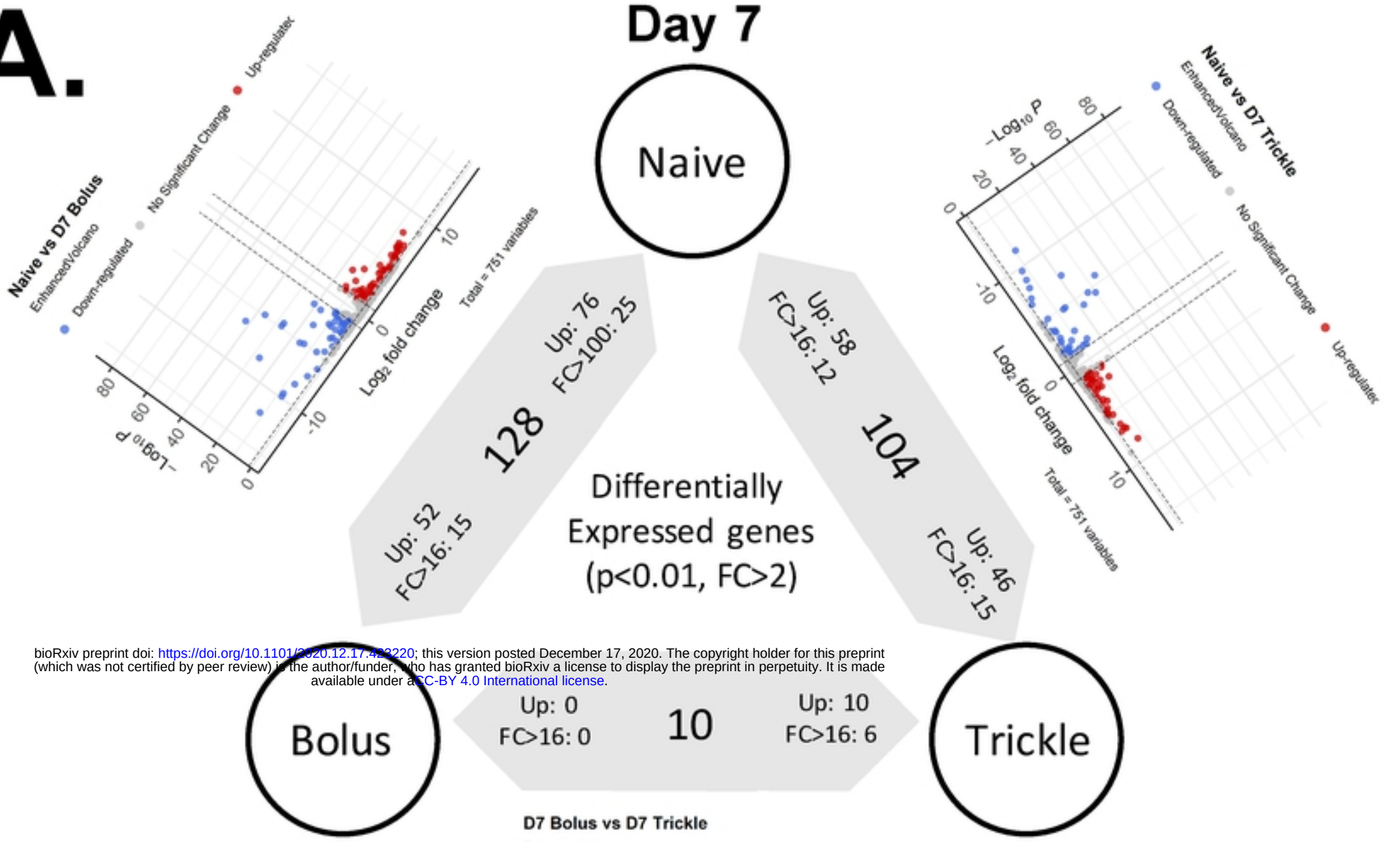

B.

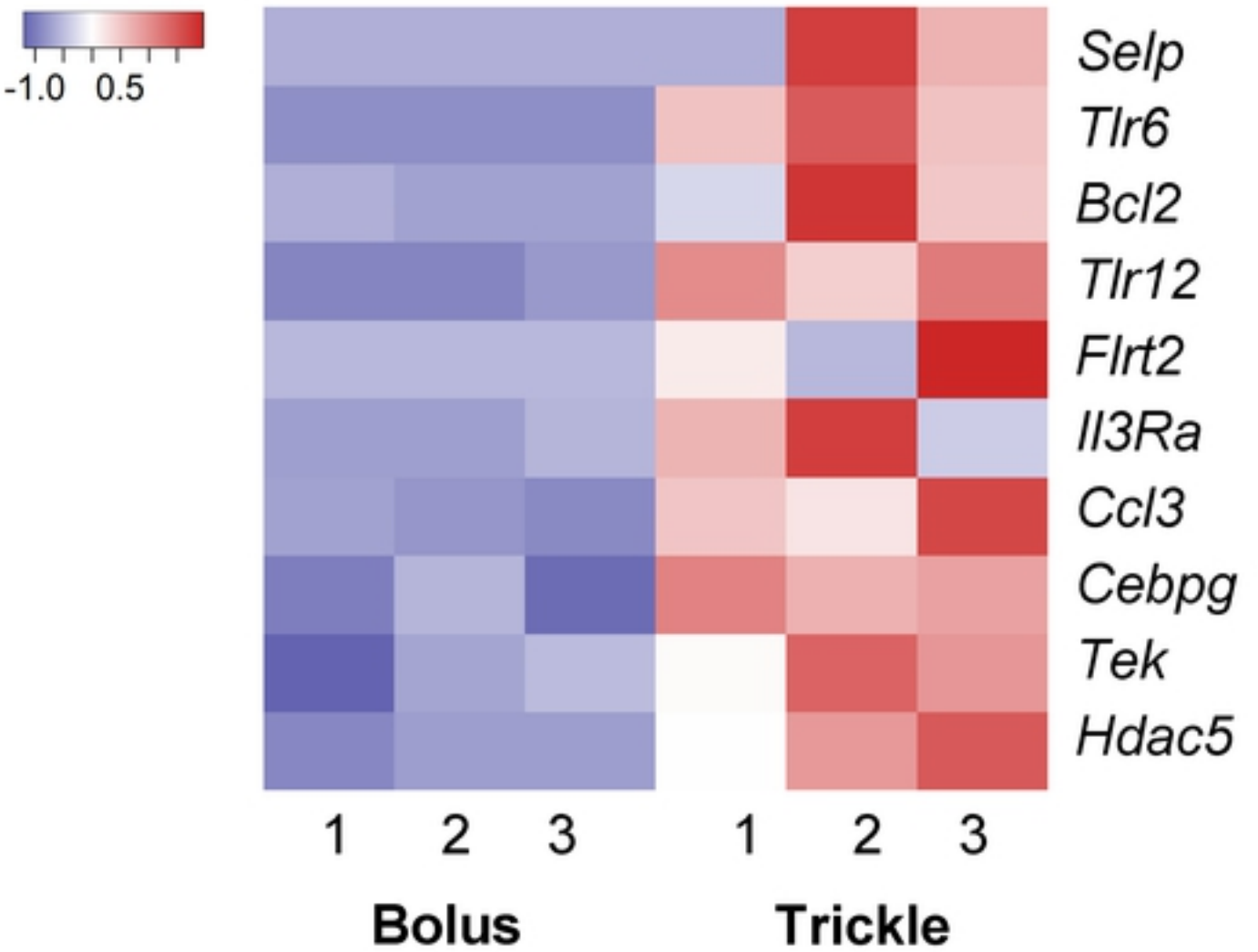

Figure 7

A.

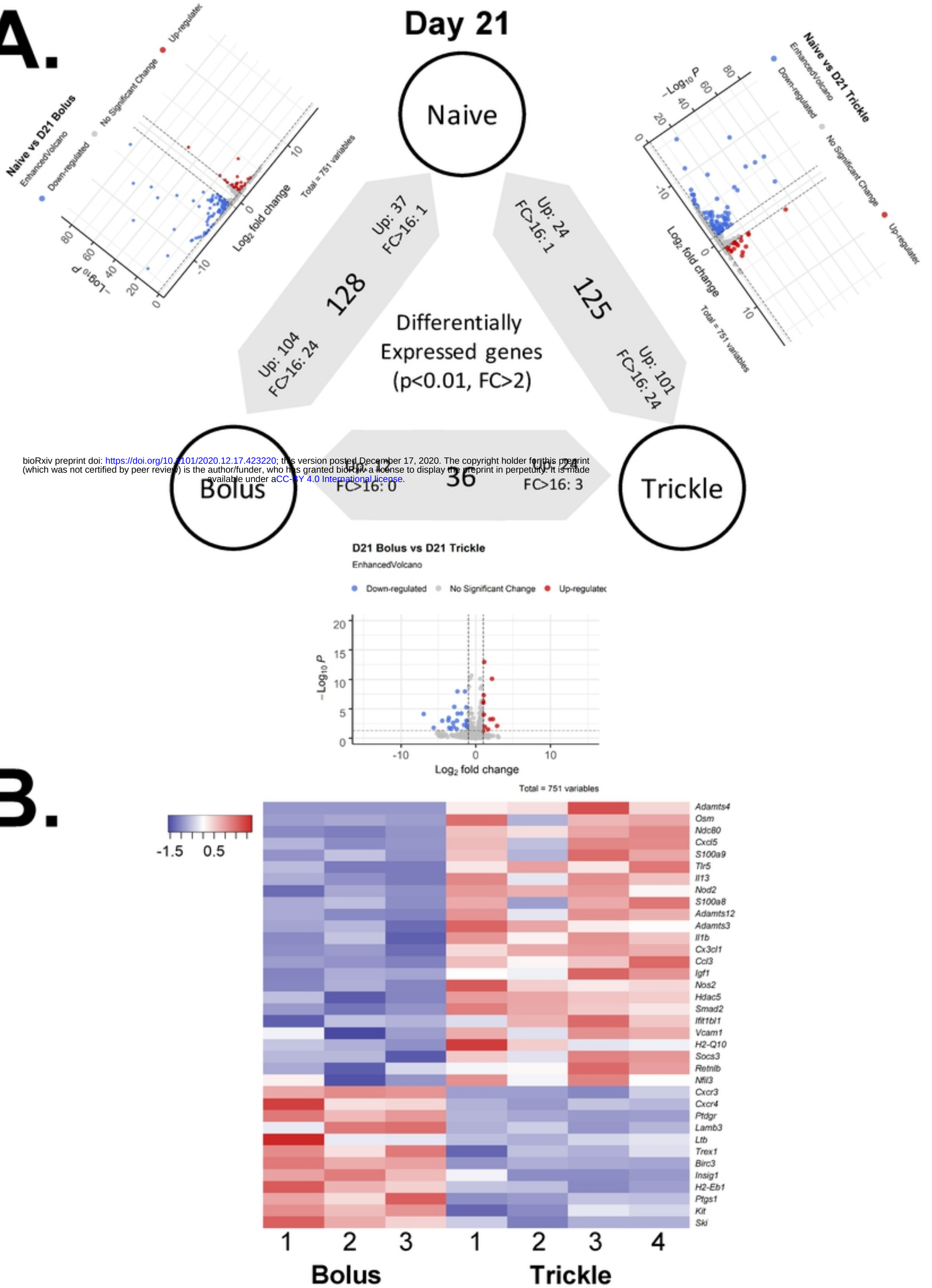

B.

Figure 8

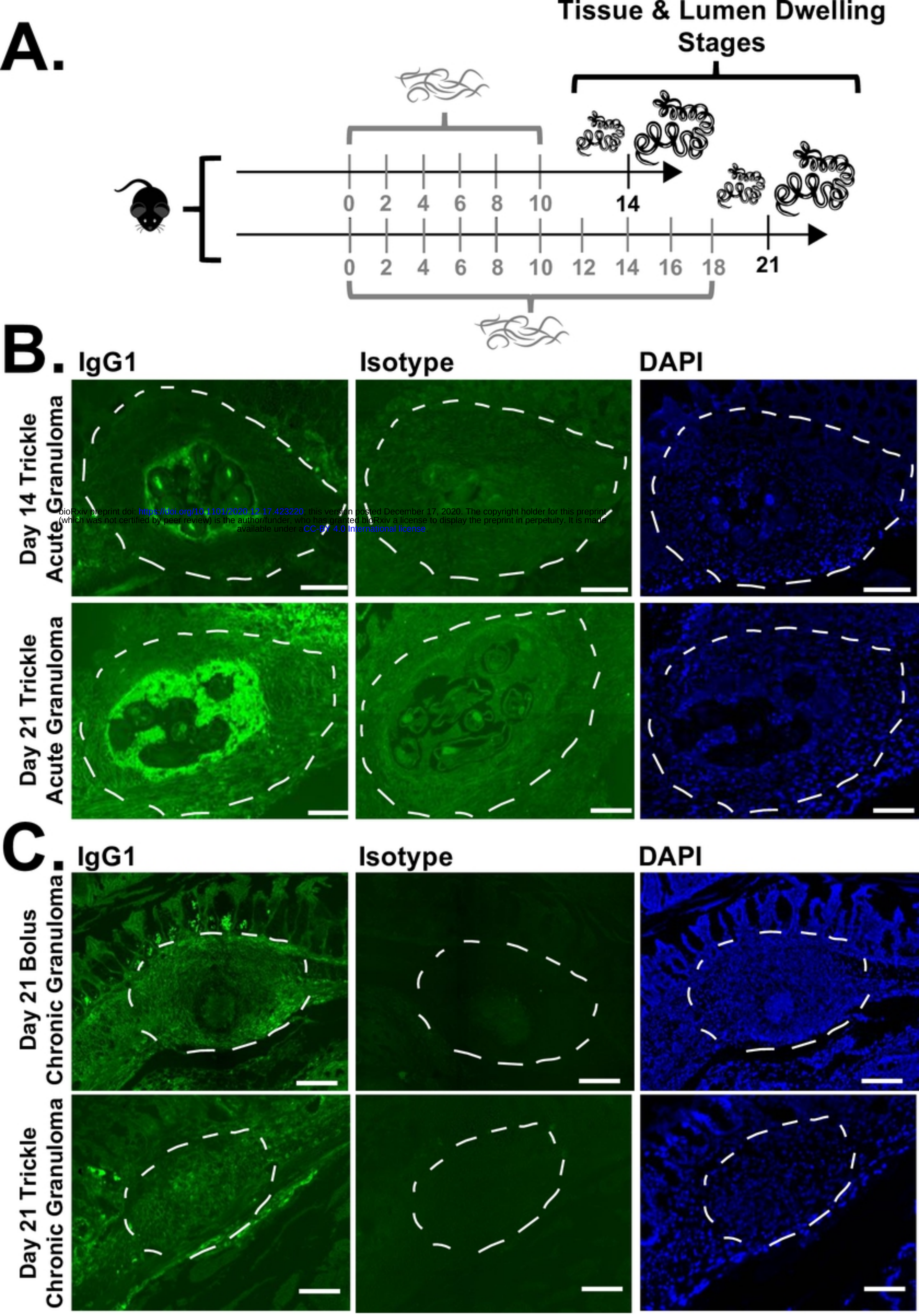

Figure 9

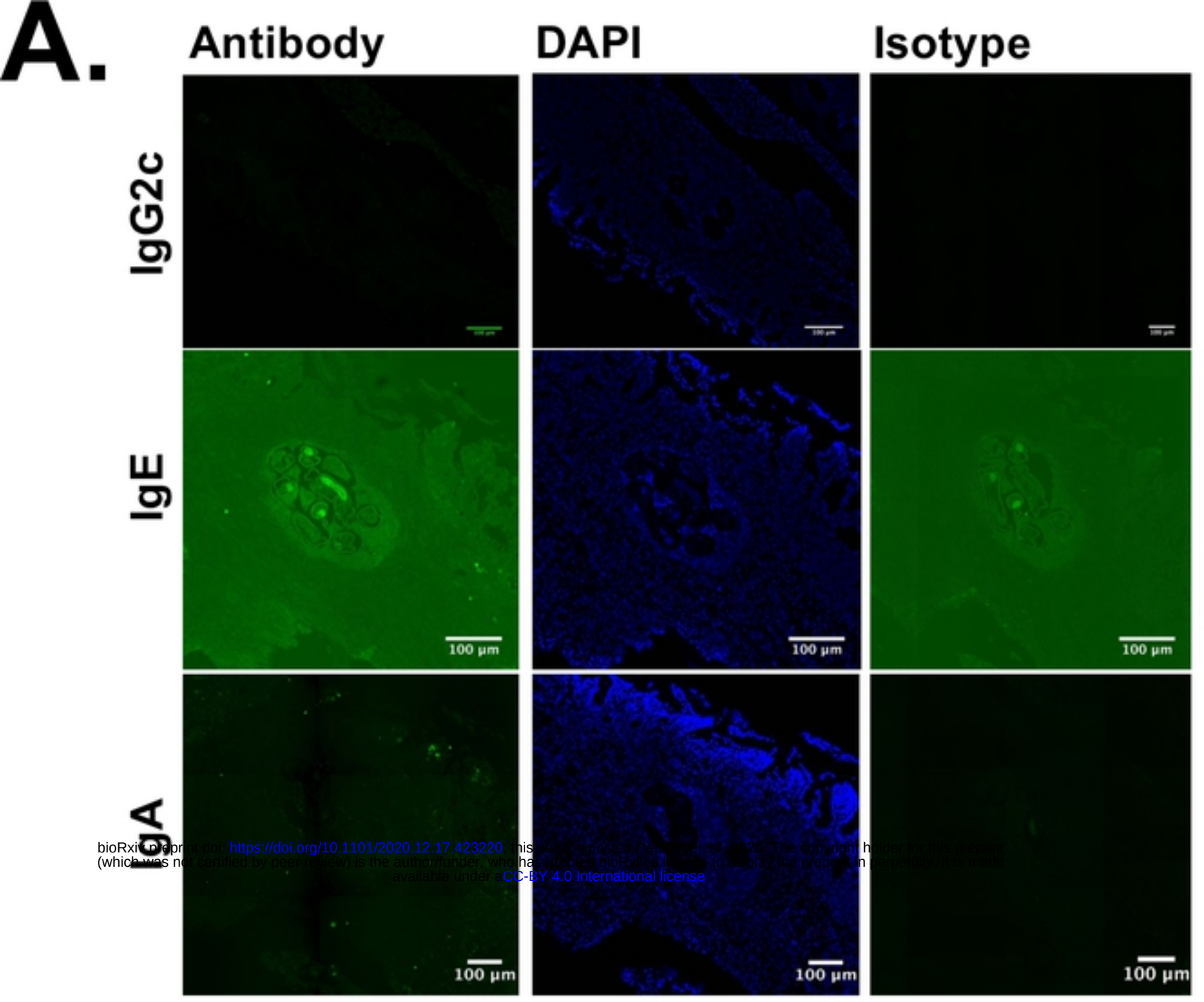

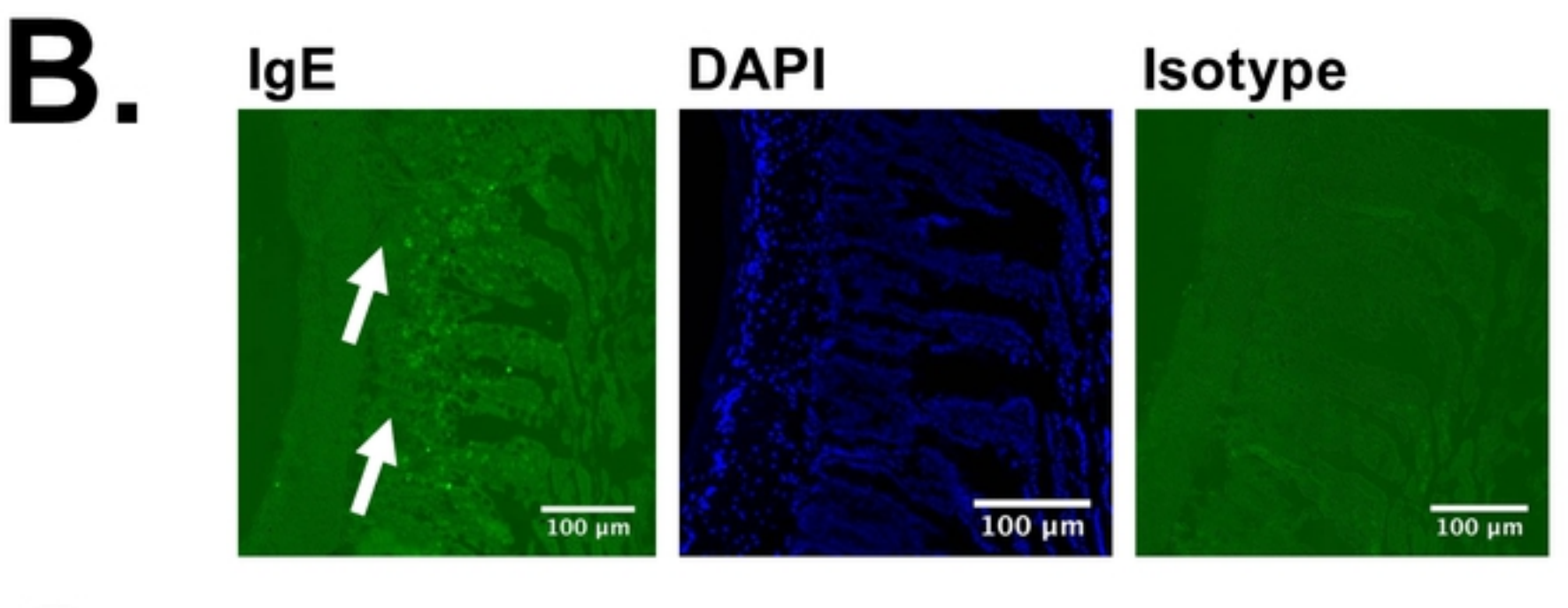

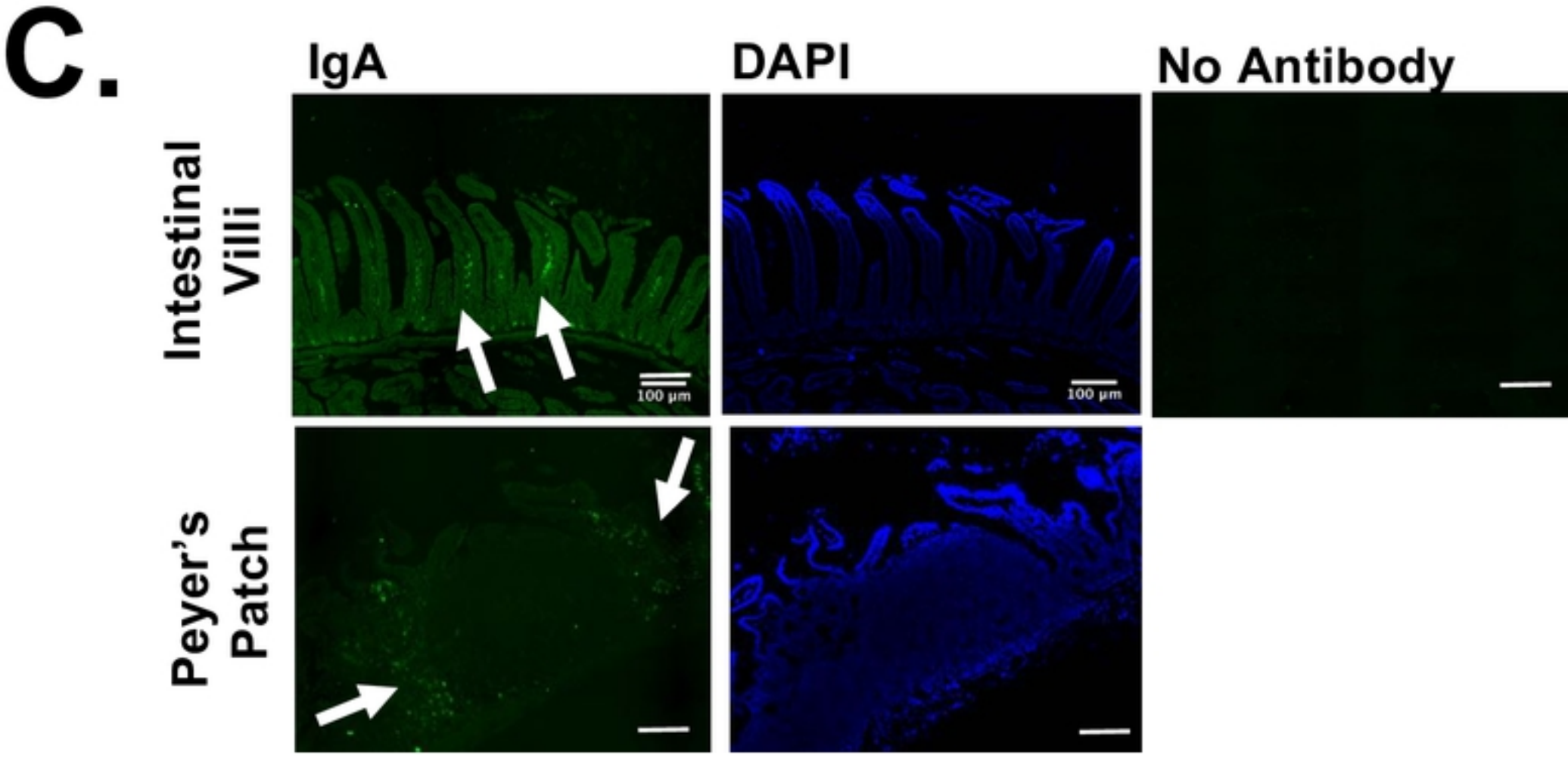

Figure 10